

Information Engineering and Technology Faculty
German University in Cairo

Development of Metamaterial Absorber

Bachelor Thesis

Authors:

Mazin N. Desouky

Supervisor:

Prof. Dr. A. M. M. A. Allam

June, 2026



Information Engineering and Technology Faculty
German University in Cairo

Development of Metamaterial Absorber

Authors:

Mazin N. Desouky

Supervisor:

Prof. Dr. A. M. M. A. Allam

June, 2026

This is to certify that:
(i) the thesis comprises only my original work toward the Bachelor Degree
(ii) due acknowledgment has been made in the text to all other material used

Mazin N. Desouky
June, 2026

Acknowledgments

Firstly, I would like to thank God for his infinite blessings in my life. Secondly, it is my pleasure to recognise the cooperation and assistance of Prof. Dr. A.M.M.A.Allam, Professor in Communication Engineering Department, Faculty of Engineering, German University in Cairo. In addition, I intend to express my gratitude to him for devoting a great deal of time, effort, and thought to this endeavour. Actually, I was fortunate to work under his supervision and I would like to thank him for his advises which have been extremely beneficial to me in gaining research experience. Finally, I would like to thank my family for their never-ending support.

Abstract

Metamaterial absorbers have attracted considerable attention due to their ability to achieve near-perfect electromagnetic absorption using artificially engineered subwavelength structures. Their unique electromagnetic properties make them promising candidates for a wide range of applications including sensing, imaging, thermal emission control, photodetection, optical filtering, and solar energy harvesting. This thesis investigates the development of optical metamaterial absorbers based on double split ring resonator (DSRR) structures and explores their potential for frequency-selective and broadband electromagnetic energy harvesting applications.

The work begins with a comprehensive review of metamaterials, metamaterial absorbers, and their operating principles across microwave, terahertz, and optical frequency regimes. In addition, selected metamaterial absorbers reported in the literature are re-simulated using CST Microwave Studio to verify the simulation methodology and establish confidence in the numerical modeling approach.

The first stage of the research focuses on the development of a geometrically scaled DSRR optical metamaterial absorber. By systematically varying the geometrical dimensions of the resonator, controlled absorption is achieved at multiple optical frequencies ranging from 423 THz to 831 THz. The obtained results demonstrate that geometrical scaling provides a predictable and efficient mechanism for resonance tuning while maintaining near-unity absorption at the desired frequencies. Furthermore, the resonance behavior is analyzed through reflection characteristics and surface current distributions, providing insight into the electromagnetic coupling mechanisms responsible for higher-order resonant modes.

Building upon these findings, the second stage introduces a wideband multi-resonance optical metamaterial absorber based on composite geometrically scaled multiple DSRRs. Composite configurations consisting of two-cell, three-cell, and four-cell resonators are investigated to study resonance interaction and bandwidth enhancement. The results demonstrate that increasing the number of coupled resonators generates additional hybrid modes, enhances resonance density, and promotes spectral overlap, gradually transforming discrete absorption peaks into a significantly broader absorption spectrum. Among the investigated configurations, the four-cell structure exhibits the strongest resonance interaction and the widest absorption bandwidth.

To evaluate the suitability of the proposed absorbers for solar-energy-related applications, a blackbody-weighted absorption analysis based on Planck's radiation law is performed. The results confirm that broadband absorption significantly improves the overlap between the absorber response and the solar blackbody radiation spectrum. The four-cell composite absorber achieves the highest blackbody-weighted absorption efficiency of 58.34 Overall, the presented work demonstrates that geometrical scaling and multi-resonator coupling provide an effective and scalable framework for engineering advanced optical metamaterial absorbers. The proposed designs successfully bridge the gap between frequency-selective absorption and broadband energy harvesting, offering promising potential for future applications in solar energy conversion, thermal photonics, optical sensing, photodetection, selective thermal emitters, and next-generation nanophotonic systems.

Contents

1 Introduction 1
1.1 Motivation 1
1.2 Thesis Organization 2
2 Review on Metamaterials and its Applications 3
2.1 Introduction 3
2.2 What are Metamaterials 4
2.2.1 Characteristics of Metamaterials 5
2.3 Metamaterial Absorbers 7
2.3.1 Basic Theory of Metamaterial Absorbers 8
2.4 Metamaterial Absorbers Applications 9
2.4.1 Microwave Frequency Absorbers 10
2.4.2 Terahertz Frequency Absorbers 12
2.4.3 Optical Frequency Absorbers 16
2.5 Chapter Summary
3 Implementation and Re-simulation of Metamaterial Absorbers 20
3.1 Introduction 20
3.2 Basic Equations 21
3.3 Re-simulation of Metamaterial Absorber in Terahertz Band 23
3.4 Development of Tunable MetaMaterial Absorber in Optical Band 27

Contents

3.4.1 Structure Design and Basic Equations 28
3.4.2 Results and Discussion 30
3.5 Chapter Summary

4 Development of Wideband Multi-Resonance Optical Metamaterial Absorber Based on Composite Geometrically Scaled Multiple DSRRs 36
4.1 Introduction 36
4.2 Structure Design and Basic Equations 38
4.3 Unit Cell Analysis 40
4.3.1 400 THz DSRR Unit Cell 41
4.3.2 640 THz DSRR Unit Cell 43
4.4 Composite Cell Analysis 45
4.4.1 Two Cell Configuration 45
4.4.2 Three Cell Configuration 47
4.4.3 Four Cells Configuration 49
4.4.4 Broadband Absorption Mechanism 51
4.4.5 Blackbody Radiation Harvesting Analysis 52
4.5 Chapter Summary

5 Conclusion and Future Work 56
5.1 Conclusion 56
5.2 Future Work 57

References 58

List of Figures

2.1 Metamaterial geometry 4
2.2 Classification of electromagnetic materials based on effective permittivity and permeability 5
2.3 Wave propagation in right-handed and left-handed materials 6
2.4 Conceptual diagram of negative refractive index in metamaterials 6
2.5 Applications of metamaterials 9
2.6 Perfect metamaterial absorber structure 10
2.7 Reflectance and absorbance of perfect metamaterial absorber 11
2.8 Schematic of a double-SRR 13
2.9 Schematic of a Π- and U-shaped THz metamaterial absorber 14
2.10 Unit cell geometry of the multi-ring terahertz metamaterial absorber 15
2.11 Absorptivity of multi-ring terahertz MTM absorber 16

List of Figures

2.12 Absorption variation of multi-ring metamaterial absorber with conductivity 17
2.13 Schematic of broadband optical metamaterial absorber 18
2.14 Absorption response of broadband optical metamaterial absorber 19
3.1 Unit cell geometry of the multi-ring terahertz metamaterial absorber 23
3.2 Absorptivity of terahertz metamaterial absorber: reference and resimulated results 24
3.3 Absorption variation of terahertz metamaterial absorber with conductivity 26
3.4 Unit cell geometry of the proposed DSRR 29
3.5 Simulated reflection coefficient and absorptivity at 423 THz and 518 THz 31
3.6 Surface current of the proposed DSRR absorber at 423 THz 32
3.7 Surface current of the proposed DSRR absorber at higher-order modes 33

List of Figures

3.8 Simulated reflection coefficient and absorptivity at 640 THz and 831 THz 34
4.1 Geometry of the proposed single DSRR unit cell 40
4.2 Reflection coefficient and absorptivity of the 400 THz unit cell 42
4.3 Reflection coefficient and absorptivity of the 640 THz unit cell 44
4.4 Geometry of the proposed two cell composite absorber 45
4.5 Reflection coefficient and absorptivity of the two cells composite absorber 46
4.6 Geometry of the proposed three cell composite absorber 47
4.7 Reflection coefficient and absorptivity of the three cells composite absorber 48
4.8 Geometry of the proposed four cells composite absorber 49
4.9 Reflection coefficient and absorptivity of the four cells composite absorber 50

List of Tables

3.1 Geometrical parameters of the proposed DSRR unit cell for different resonance frequencies 30
3.2 Comparison with previous works 35
4.1 Geometrical parameters of the 400 THz unit cell 41
4.2 Geometrical parameters of the 640 THz unit cell 43
4.3 Geometrical parameters of the two cell configuration 45
4.4 Geometrical parameters of the three cell configuration 47
4.5 Geometrical parameters of the four cells configuration 49
4.6 Blackbody-weighted absorption efficiency of the investigated configurations 53

List of Abbreviations

CST	Computer Simulation Technology
CSRR	Circular Split Ring Resonator
DNG	Double Negative
DSRR	Double Split Ring Resonator
EM	Electromagnetic
ENG	Epsilon Negative
FDTD	Finite Difference Time Domain
GHz	Gigahertz
IR	Infrared
LHM	Left-Handed Material
MMA	Metamaterial Absorber
MTM	Metamaterial
RF	Radio Frequency
RCS	Radar Cross Section
RHM	Right-Handed Material
SRR	Split Ring Resonator
THz	Terahertz
UAV	Unmanned Aerial Vehicle
UV	Ultraviolet
VO_2	Vanadium Dioxide

List of Symbols

$A(\omega)$	Absorption coefficient
A_{BW}	Blackbody-weighted absorption
c	Speed of light in vacuum
E	Electric field intensity
f	Frequency
h	Planck constant
H	Magnetic field intensity
k_B	Boltzmann constant
n	Refractive index
P	Power density
$R(\omega)$	Reflection coefficient
S_{11}	Reflection scattering parameter
S_{21}	Transmission scattering parameter
T	Absolute temperature
$T(\omega)$	Transmission coefficient
λ	Wavelength
μ	Permeability
μ_r	Relative permeability
ε	Permittivity
ε_r	Relative permittivity
ω	Angular frequency

Chapter 1

Introduction

1.1 Motivation

Metamaterials are artificially engineered electromagnetic structures that exhibit properties not readily available in naturally occurring materials. Their ability to manipulate electromagnetic waves has enabled the development of numerous devices with enhanced performance, including antennas, sensors, filters, lenses, cloaking devices, and electromagnetic absorbers. Among these applications, metamaterial absorbers have attracted significant attention due to their capability of achieving very high absorption while maintaining compact dimensions.

Since the introduction of the first near-perfect metamaterial absorber by Landy et al., extensive research has been conducted to improve absorption performance across microwave, terahertz, infrared, and optical frequency ranges. Optical metamaterial absorbers are particularly important because of their potential applications in photodetection, thermal imaging, optical filtering, sensing, thermal emission control, and solar energy harvesting. Their electromagnetic response can be controlled through the careful design of subwavelength resonant structures, allowing the absorption characteristics to be tailored for specific applications.

One of the major challenges in optical metamaterial absorber design is the limited bandwidth of conventional resonant structures. Although near-unity absorption can be achieved at specific frequencies, many absorbers operate over relatively narrow frequency ranges, which limits their effectiveness for broadband applications. Solar energy harvesting represents one of the most important examples where broad spectral coverage is required in order to maximize the utilization of incident radiation.

The resonance characteristics of metamaterial absorbers are strongly dependent on the geometry of the resonant elements. Therefore, geometrically scalable resonators provide a promising approach for controlling resonance frequencies and developing absorbers with enhanced spectral performance. In addition, combining multiple resonators within a

single structure can introduce resonance interaction and spectral overlap, which may lead to significantly wider absorption bandwidths.
This thesis investigates the development of optical metamaterial absorbers based on double split ring resonator (DSRR) structures. The work focuses on two main objectives. The first objective is the development of a geometrically scaled DSRR absorber capable of achieving controlled absorption at multiple optical frequencies. The second objective is the development of a wideband optical absorber through the integration of multiple geometrically scaled DSRRs within composite unit-cell configurations. Furthermore, the suitability of the proposed structures for solar energy harvesting applications is evaluated through blackbody-weighted absorption analysis.

1.2 Thesis Organization

This thesis is divided into five chapters including this chapter.
Chapter 2 presents a literature review on metamaterials, metamaterial absorbers, and their applications. The chapter discusses the fundamental concepts of metamaterials, absorption mechanisms, optical metamaterial absorbers, and solar energy harvesting. In addition, several previously reported absorber structures are reviewed and compared.
Chapter 3 presents the implementation and re-simulation of selected metamaterial absorbers reported in the literature. The chapter also introduces the development of a geometrically scaled optical DSRR absorber and investigates its resonance characteristics and absorption performance.
Chapter 4 presents the development of a wideband multi-resonance optical metamaterial absorber based on composite geometrically scaled multiple DSRRs. Different composite configurations are analyzed to investigate resonance interaction, bandwidth enhancement, and blackbody-radiation harvesting performance.
Chapter 5 presents the conclusions of the thesis and summarizes the main findings of the work. In addition, recommendations and possible future research directions are discussed.

Chapter 2

Review on Metamaterials and its Applications

2.1 Introduction

In recent years, energy harvesting has assumed an increasingly important role across various technological fields. Solar cells, for instance, have been widely employed to harvest energy by converting visible and ultraviolet light from sunlight into electricity. Similarly, energy harvesting from water pipelines has enabled sensors to generate power from the motion of flowing water. More recently, metamaterials have emerged as a promising technology for capturing ambient electromagnetic waves (RF/microwave) and rectifying them into usable electrical energy. As a result, there is a growing need for effective materials and techniques to control and mitigate the impact of unwanted EM waves. One practical solution to this problem is the use of electromagnetic absorbers, which are designed to absorb incident wave energy while minimizing reflection and interference [1, 2]. This necessity has motivated the development of metamaterial absorbers, which have attracted significant attention for their ability to achieve near-perfect absorption of electromagnetic waves by engineering subwavelength structures with tailored electric and magnetic responses.

The concept of metamaterials was first introduced theoretically by V. G. Veselago in 1967, who predicted that materials with simultaneously negative permittivity (ε) and permeability (μ) would exhibit unusual electromagnetic properties, including a negative refractive index and reversed wave propagation phenomena [3]. This idea remained theoretical until J. B. Pendry and his colleagues proposed practical artificial structures to realize such properties in 1996 [4]. In 1998, Pendry introduced periodic thin metallic wire arrays that exhibited plasma-like behavior and enabled negative effective permittivity at microwave frequencies [5]. Later, in 1999, he developed the split ring resonator (SRR), a subwavelength structure capable of producing negative effective permeability [6]. By com-

bining these two elements, D. R. Smith and collaborators successfully demonstrated the first composite metamaterial with simultaneously negative permittivity and permeability in 2000, marking the first experimental realization of a negative-index (left-handed) medium and establishing the foundation for modern metamaterial research [7]. Metamaterial structures can be designed in two-dimensional or three-dimensional periodic forms and can exhibit unusual electromagnetic characteristics such as negative refractive index, left-handed behavior, cloaking, and perfect absorption [8–11].

One of the most challenging applications of metamaterial absorbers is the continuous powering of unmanned aerial vehicles (UAVs). Among various types of ambient energy sources, electromagnetic waves represent a promising candidate for charging UAVs through adaptive beamforming steering during mission execution, potentially eliminating the need to land at power stations for recharging.

This chapter presents a comprehensive investigation of metamaterial absorber design principles and their various applications, with particular emphasis on systems relevant to UAVs. The study examines how metamaterial absorbers can be utilized for electromagnetic energy harvesting to support UAV charging applications, along with other key functions including frequency-selective absorption and sensing. Representative implementations are analyzed, and future research directions for integrating metamaterial absorbers into UAV power systems are discussed.

2.2 What are Metamaterials

Metamaterial (MTMs) structures are artificially engineered electromagnetic structures that control electromagnetic waves through their physical shape and arrangement rather than through only their intrinsic material properties. The term has been widely used following formal definitions in the literature [12]. These structures are typically composed of small repeating elements (unit cells) whose dimensions are much smaller than the wavelength of the incident electromagnetic wave, allowing the overall structure to be treated as an effective medium. Metamaterials can be realized as two-dimensional or three-dimensional periodically designed macroscopic composites that display exotic properties extending from microwave to optical frequency ranges [13].

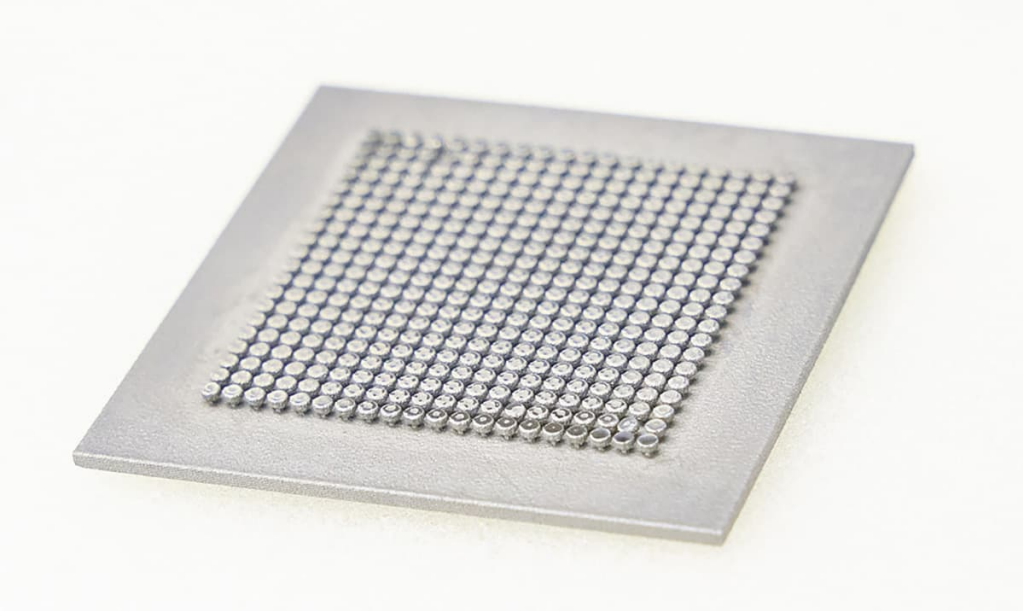


Figure 2.1: Metamaterial geometry [14]

The first metamaterial absorber was introduced by Landy et al. [15], demonstrating a compact structure with high absorption performance. Since then, many designs have been developed to achieve multiband, broadband, polarization-insensitive, and tunable absorption for applications ranging from microwave to optical frequencies [16–21]. Despite these advances, achieving high efficiency across multiple frequency bands while maintaining stable performance remains a challenge.

In conventional materials, electromagnetic behavior is mainly determined by inherent material properties such as permittivity, permeability, and refractive index. In contrast, metamaterials obtain their electromagnetic response from the combined effect of their structural elements, which can be carefully designed to achieve specific wave interaction at selected frequencies. This enables properties that do not exist naturally in conventional materials, including negative refractive index and near-perfect absorption [13]. From an engineering point of view, metamaterials can be considered electromagnetic structures in which geometry plays a key role in shaping how waves propagate, reflect, or are absorbed.

2.2.1 Characteristics of Metamaterials

Metamaterials possess a set of characteristics that distinguish them from conventional electromagnetic materials. By properly designing the geometry and arrangement of the unit cells, metamaterials can be tailored to exhibit specific electromagnetic responses within a chosen frequency range. One of the key characteristics of metamaterials is their subwavelength unit-cell size, which allows the structure to be treated as an effective medium and enables controlled interaction with electromagnetic waves without significant diffraction effects.

As shown in Fig. 2.2, the effective permittivity and permeability of metamaterial structures may be negative, corresponding to different quadrants of the ε–μ plane [13]. Media with $\varepsilon < 0$ and $\mu > 0$ are termed epsilon-negative (ENG) (plasma-like) materials. Media with $\varepsilon > 0$ and $\mu < 0$ are sometimes associated with gyrotropic magnetic responses. Media with both $\varepsilon < 0$ and $\mu < 0$ are termed double-negative (DNG) metamaterials and can be realized artificially; in such media, the direction of wave propagation can be reversed as shown in Fig. 2.3 [13]. In addition, the refractive index can be negative compared to conventional materials, as illustrated in Fig. 2.4 [14].

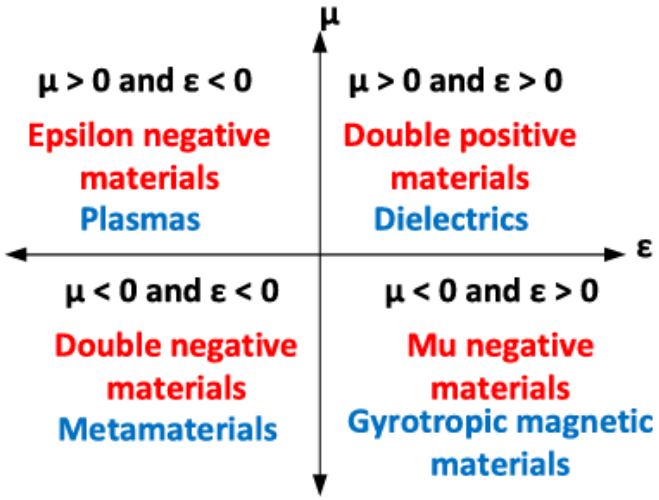


Figure 2.2: Classification of electromagnetic materials based on the signs of effective permittivity (ε) and permeability (μ) [13].

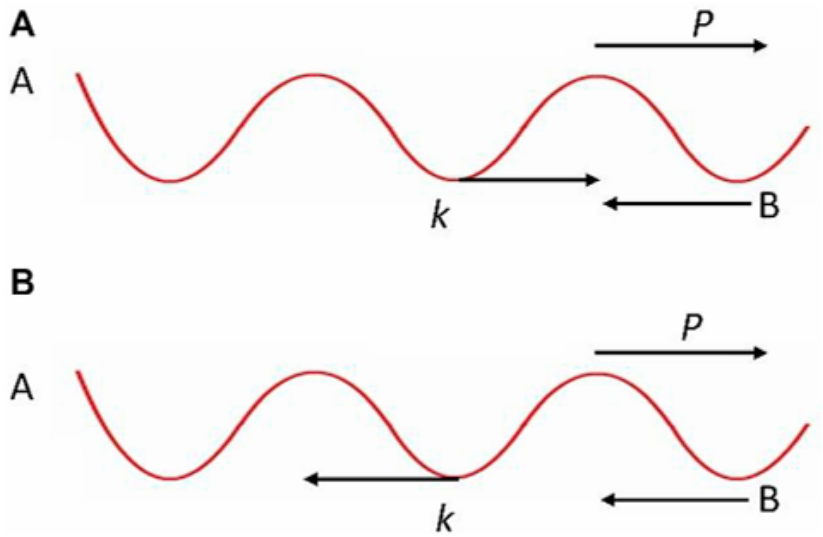


Figure 2.3: Wave propagation in (A) right-handed materials (RHM) and (B) left-handed materials (LHM) [13].

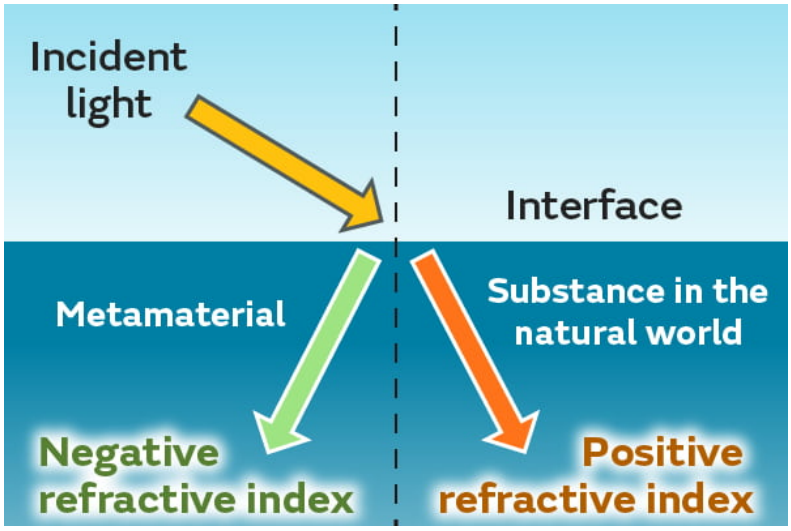


Figure 2.4: Conceptual diagram of negative refractive index in metamaterials [14].

Another important characteristic is the ability of metamaterials to produce resonant electromagnetic behavior. Metallic patterns and dielectric layers form resonant circuits that interact with the electric and magnetic fields of the incident wave, and these resonances strongly influence operating frequency and bandwidth. Metamaterials also offer design flexibility, since the electromagnetic response can be modified by adjusting geometric parameters such as shape, size, spacing, and orientation of the unit cells.
Additionally, metamaterials can be designed to exhibit polarization and angle stability. Symmetric unit-cell structures allow the electromagnetic response to remain nearly unchanged under different polarization angles and incident directions, which is desirable for practical applications.

2.3 Metamaterial Absorbers

Metamaterial absorbers are artificially engineered structures designed to achieve near-perfect absorption of electromagnetic waves at specific frequencies. They operate by tailoring the effective permittivity and permeability of subwavelength unit cells to match the impedance of free space, thereby minimizing reflection while dissipating the incident energy as loss within the structure. The absorption performance is controlled by the coupling effects between resonant elements. By adjusting geometry, spacing, substrate properties, and unit cell dimensions, the resonant behavior and absorption characteristics can be tuned.
Overall, extensive research has been conducted to develop metamaterial absorbers across different frequency regimes, from microwave to optical bands, providing a broad understanding of the design principles and performance characteristics of MMAs for various electromagnetic applications [13].

2.3.1 Basic Theory of Metamaterial Absorbers

Metamaterial absorbers attenuate incident EM waves by converting electromagnetic en ergy into other forms, primarily thermal energy. Such materials are essential in applica tions including electromagnetic compatibility, high-efficiency energy harvesting, sensing platforms, and stealth technology. MMAs are also called a perfect absorber with near unity absorption, showing zero reflection and transmission coefficients for plane waves that are typically incident [13]. Metamaterial absorber consists of three main layers. The top layer contains a patterned metallic structure that acts as a resonator, the mid dle layer is a dielectric substrate, and the bottom layer is a continuous metallic ground plane, the ground plane prevents transmission of electromagnetic waves, so the absorption performance mainly depends on minimizing the reflected power. The absorption of a metamaterial absorber is determined by

$$A = 1 - |S_{11}|^2 - |S_{21}|^2 \tag{2.1}$$

Since the ground plane blocks transmission ($S_{21} \approx 0$), near-perfect absorption can be achieved by minimizing the reflection coefficient (S_{11}) [15]. Conventional absorbers often require large thicknesses and multilayer configurations, which limit their applicability in compact and lightweight systems [22]. This limitation has motivated researchers to explore alternative solutions. Metamaterial absorbers can be designed in various geometrical shapes according to the desired application, which has significantly increased their attractiveness and demand. Metamaterial absorbers have been widely investigated for electromagnetic wave absorption over a broad range of frequencies, extending from the microwave region to the optical spectrum. The operating frequency of a metamaterial absorber mainly depends on the geometry of the unit cell, substrate properties, and the dimensions of the resonator elements. Consequently, numerous designs have been proposed in the literature to achieve high absorption at specific frequency bands.

2.4 Metamaterial Absorbers Applications

This section summarizes representative metamaterial absorber implementations operating at different frequency bands including microwave, terahertz, and optical regions as illustrated at (Fig. 2.5) [13].The selected designs are analyzed and evaluated using CST Microwave Studio, which is a full-wave electromagnetic simulation tool based on numerical methods. The purpose of this section is to demonstrate how the electromagnetic performance of metamaterial absorbers can be controlled through structural design and material selection. For each frequency band, representative unit-cell geometries reported in the literature are modeled and simulated in CST in order to obtain their reflection coefficient, transmission coefficient, and absorption characteristics.

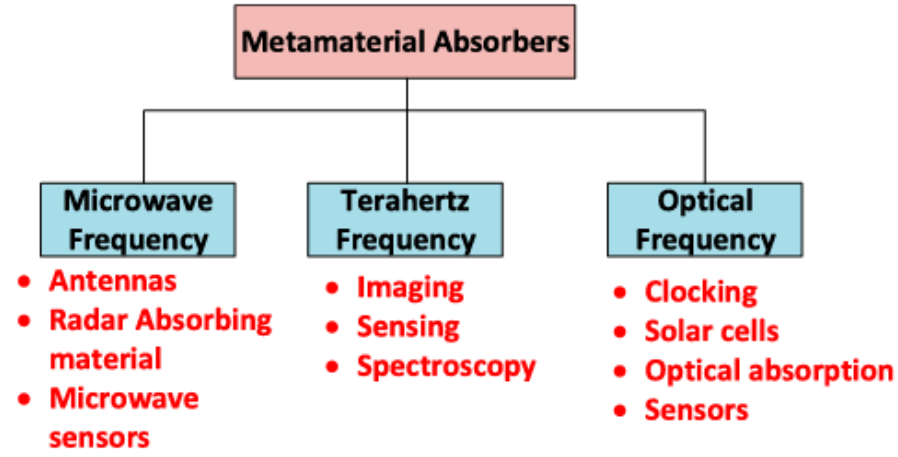


Figure 2.5: Applications of metamaterials [13].

2.4.1 Microwave Frequency Absorbers

The microwave region (1 GHz to 30 GHz) is widely studied due to applications in radar systems, wireless communication, and stealth technology. A typical microwave metamaterial absorber consists of a periodic metallic resonator printed on a dielectric substrate with a continuous metallic ground plane. The ground plane eliminates transmission, while the resonator is designed to minimize reflection through impedance matching with free space.

There are various applications in this band such as Radar-Cross Section (RCS). Radar cross section (RCS) is a measure of how detectable an object is by radar systems. It represents the amount of electromagnetic energy reflected back toward the radar receiver when a target is illuminated by an incident wave. A metamaterial structure designed for radar cross-section (RCS) reduction was presented in a previous study, where near-perfect absorption was achieved by Landy et. al [24]. The design is based on a split-ring resonator connected through an inductive strip to a transmission line located on the opposite side of the substrate, as shown in Fig. 2.6. By properly selecting the resonator geometry and the substrate thickness, the structure allows separate tuning of the electric and magnetic resonances. As a result, both the electric and magnetic components of the incident electromagnetic wave are effectively absorbed.

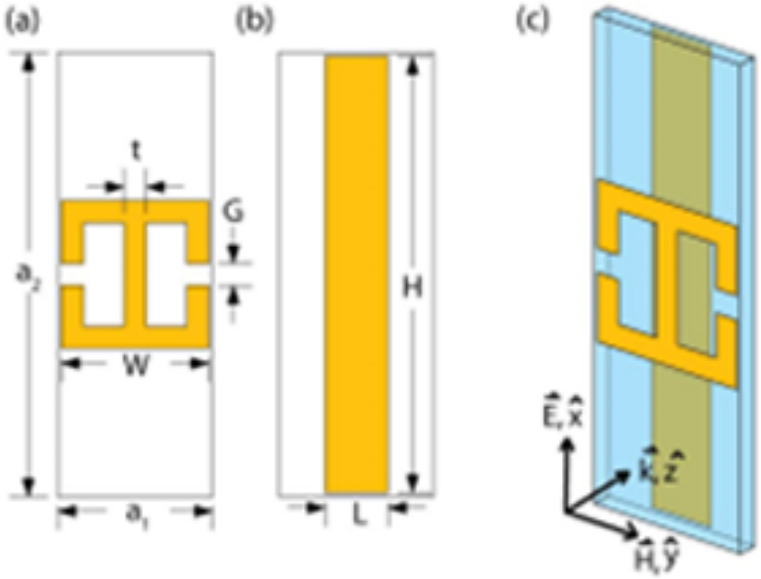


Figure 2.6: Perfect metamaterial absorber: (a) top, (b) bottom, and (c) 3D view [24].

Simulation and experimental results indicate that reflectance $R(\omega)$ and transmittance $T(\omega)$ are minimized near resonance, producing high absorption $A(\omega)$ around 11.5 GHz (Fig. 2.7) [24].

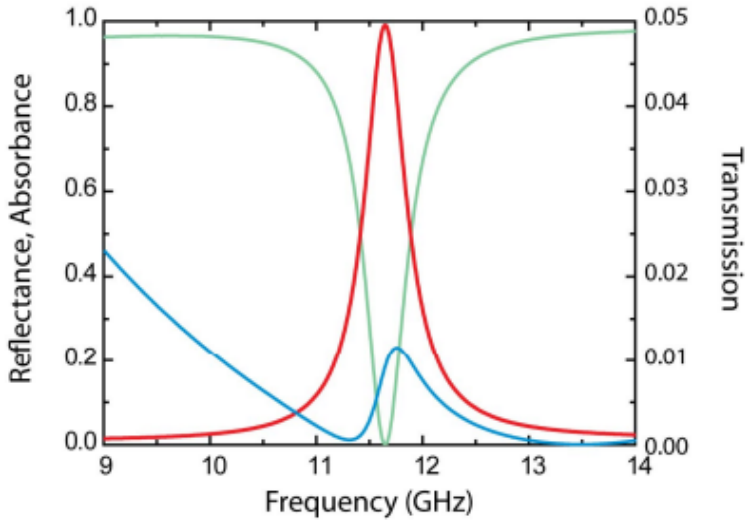


Figure 2.7: Reflectance and absorbance [24].

2.4.2 Terahertz Frequency Absorbers

The terahertz (THz) frequency domain, which ranges from 1 to 10 THz, is located between the microwave and infrared (IR) frequency regions. THz metamaterial absorbers (MMAs) have recently attracted significant research interest due to their potential applications in imaging and spectroscopy, the non-ionizing nature of THz radiation, and their ability to penetrate materials such as plastics, paper, and fabrics. Initially, metamaterial absorbers were primarily developed for operation in the microwave frequency range because fabrication at these frequencies is relatively straightforward. However, with the advancement of design methodologies and fabrication technologies, their operation has been extended to cover a much wider frequency spectrum. By adjusting the geometrical parameters of the unit cell, metamaterial absorbers can now be designed to operate from the microwave region through the terahertz band and even into the visible frequency range.

This design flexibility represents one of the main advantages of metamaterials, as it enables researchers to explore and develop devices operating within the terahertz region, which has traditionally been difficult to exploit and is often referred to as the "THz gap." Various THz absorber configurations have been investigated, including fishnet structures [25–27], SRR-based designs [28–30], U-shaped resonators [31, 32], chiral structures [33], and graphene-based metamaterial absorbers [34–41].

Tao et al. [42] demonstrated a THz metamaterial absorber based on SRR arrays, as illustrated in Fig. 2.8. The reported absorption peaks were attributed to a combination of LC resonance and higher-order dipole modes, with absorption approaching 0.96 near 1.6 THz [42].

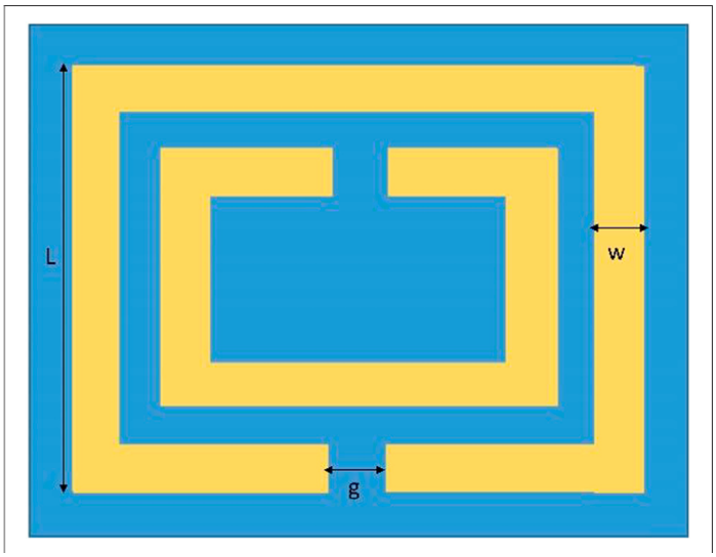


Figure 2.8: Schematic of a double-SRR [13].

Wang et al. [43] proposed a dual-band THz metamaterial absorber based on a U-shaped

metallic resonator, as illustrated in Fig. 2.9. The proposed design achieved two absorption peaks near 1.80 THz and 2.97 THz, both exceeding 98% absorption [43].
Mohanty et al. [44] proposed a multiband THz metamaterial absorber combining Π-shaped and U-shaped resonator elements, as shown in Fig. **??**. The reported structure exhibited three distinct absorption peaks with an average absorption close to 97%, demonstrating the effectiveness of combining multiple resonator geometries to achieve multiband absorption characteristics [44].

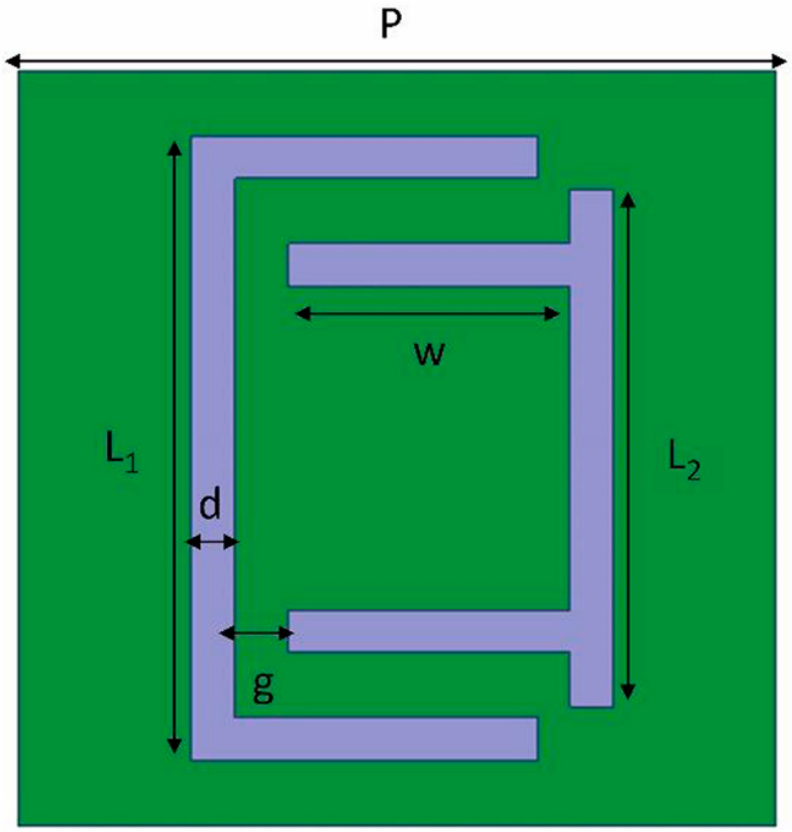


Figure 2.9: Schematic of a Π- and U-shaped THz metamaterial absorber [44].

An ultra-wideband tunable metamaterial absorber operating in the terahertz frequency range was proposed in. [52]. The unit cell consists of three concentric resonance rings made of vanadium dioxide (VO_2) placed over a dielectric spacer and backed by a metallic ground plane. The dielectric layer is silicon dioxide (SiO_2), while the bottom metallic layer eliminates transmission as presented in Fig. 2.10. The multi-ring structure enables the excitation of multiple resonant modes, which combine to achieve broadband absorption. The symmetric geometry also provides polarization-insensitive performance.

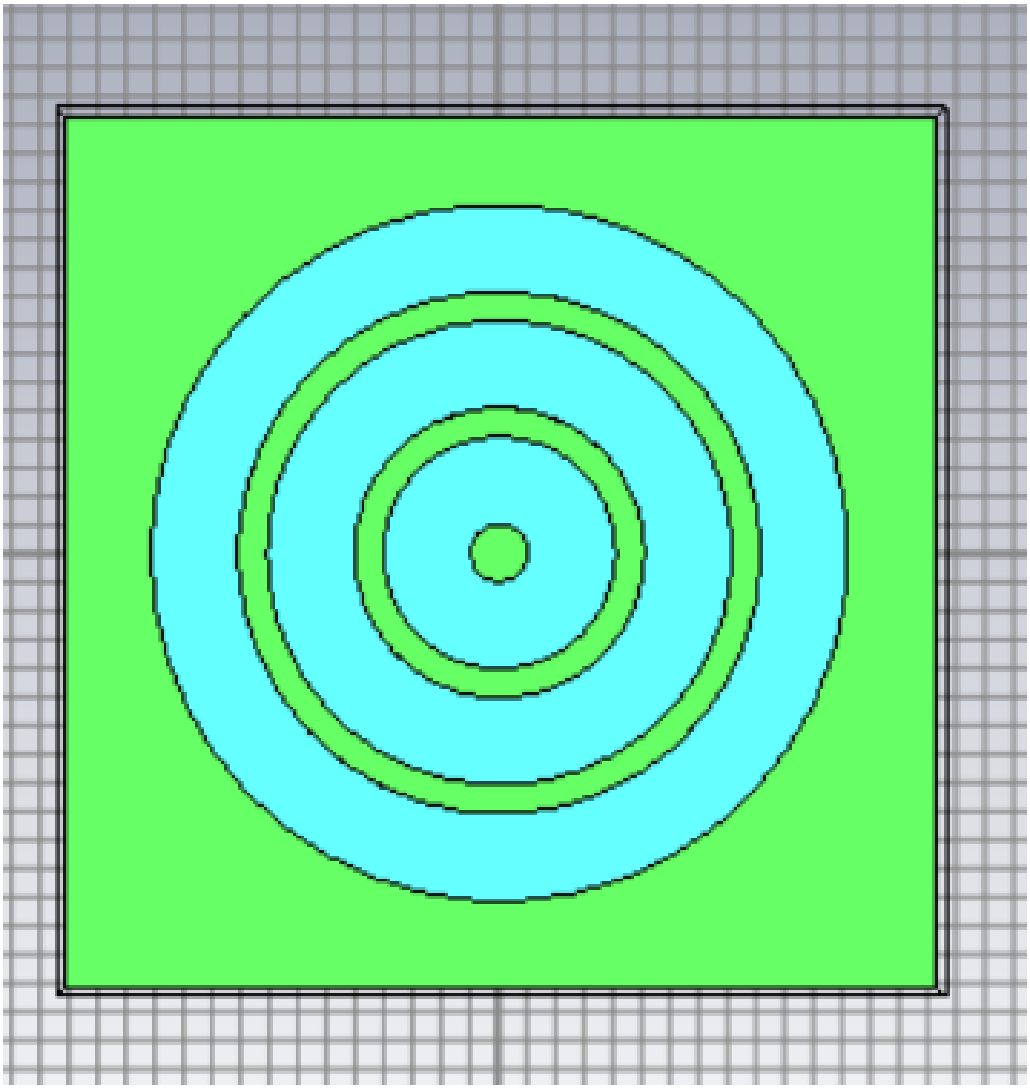


Figure 2.10: Unit-cell geometry of a multi-ring terahertz metamaterial absorber [26].

The reported results demonstrate excellent absorption performance, where the absorptivity exceeds 90% over a wide frequency range from approximately 2.34 THz to 5.64 THz. Two main absorption peaks are observed around 2.83 THz and 5.19 THz as illustrated in (Fig. 2.11) [52], and the high absorption is achieved through impedance matching with free space and destructive interference inside the structure. Since the ground layer blocks transmission, the absorption is calculated using:

$$A(\omega) = 1 - |S_{11}|^2 \tag{2.2}$$

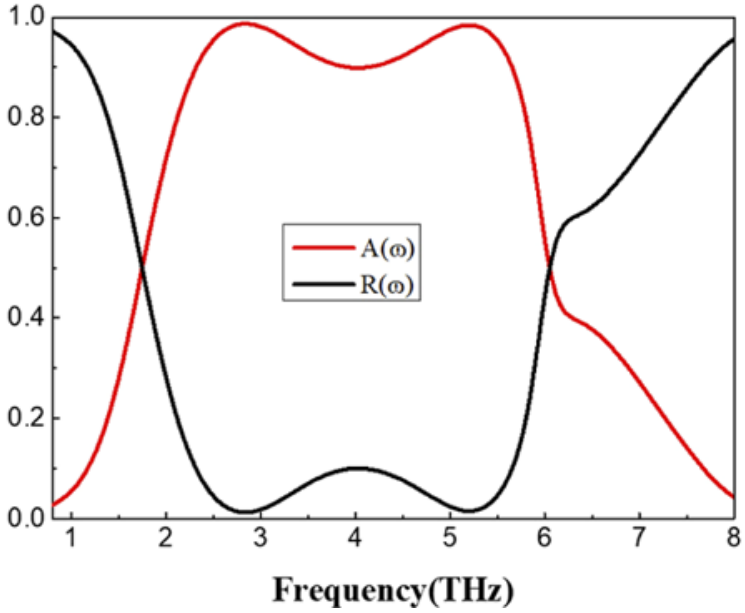


Figure 2.11: Absorbitivity of multi-ring terahertz MTM absorber [52].

In addition to broadband operation, the absorber exhibits dynamic tunability by controlling the electrical conductivity of the VO_2 layer. As the conductivity varies from 200 S/m (insulating state) to 2×10^5 S/m (metallic state), the absorption intensity increases continuously from approximately 4% to nearly perfect absorption, while the operating frequency band remains almost unchanged as presented in (Fig. 2.12). The absorber also demonstrates polarization-insensitive behavior and wide-angle performance, making it suitable for various terahertz applications such as sensing, imaging, modulation, and stealth technologies [52].

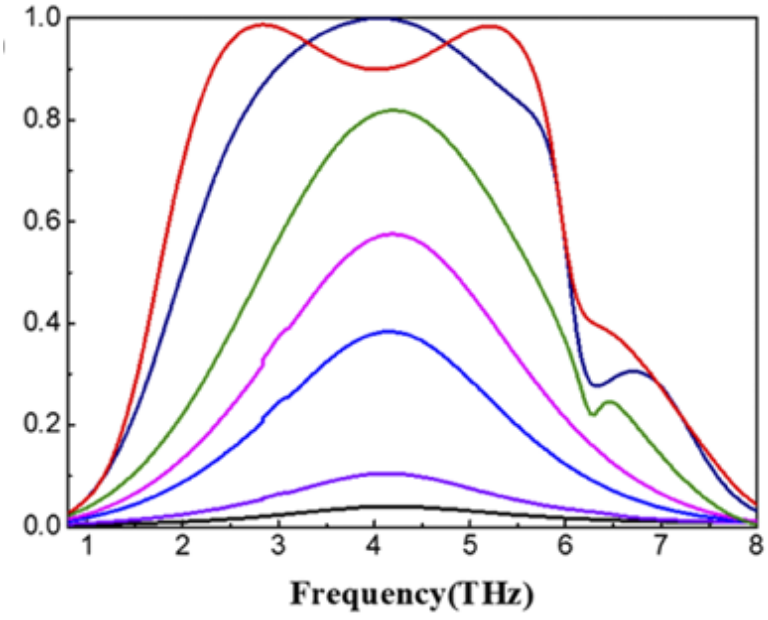


Figure 2.12: Absorbtion variation of multi-ring MTM absorber with conductivity ([52].

2.4.3 Optical Frequency Absorbers

Optical metamaterial absorbers are designed to operate in optical and mid-infrared regimes, where unit-cell dimensions must be on the nanometer scale, requiring advanced nanofabrication. Despite this challenge, optical and mid-IR MMAs are of high interest for applications such as thermal emission control and energy harvesting [45–49]. Avitzour et al. [50] reported an early metamaterial-based absorber in the IR region with absorption exceeding 90% and near-zero reflectivity.

Bossard et al. [51] proposed a broadband optical metamaterial absorber that is polarization-insensitive and provides a super-octave bandwidth (Fig. 2.13). Near-unity absorption was achieved by optimizing the geometry to support overlapping resonant modes across the operating band, with stable absorption over incident angles up to 45° (Fig. 2.14) [51].

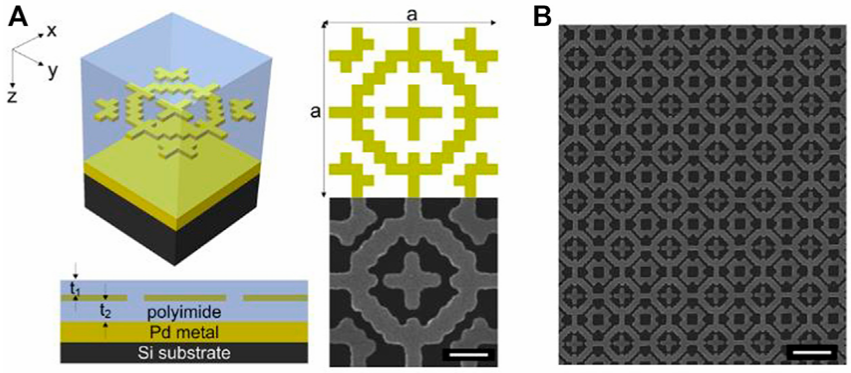


Figure 2.13: (A) Schematic of the unit cell broadband absorber. (B) Nanofabricated image [51].

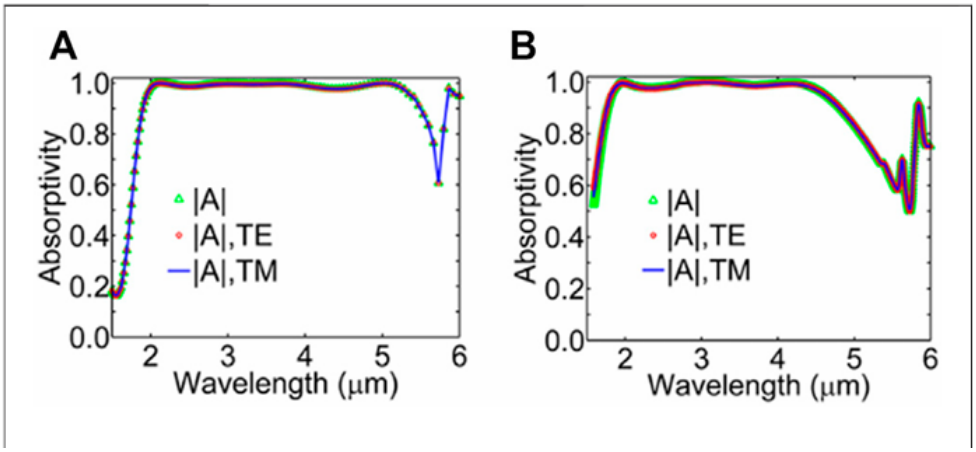


Figure 2.14: (A) Simulated and (B) measured absorptivity [51].

2.4.4 Plasmonic Metamaterial Absorbers for UAV Energy Harvesting

In the terahertz and optical regimes, metamaterial absorbers have attracted attention for autonomous energy harvesting applications in unmanned aerial vehicles (UAVs). The dual-band circular split-ring resonator (CSRR) absorber proposed by Alawad et al. [52], originally designed in the microwave region, can be geometrically scaled to nanometer dimensions to operate in the plasmonic frequency band, since the resonance frequency of metamaterial structures is inversely proportional to their physical size. When implemented using plasmonic metals such as silver or graphene on dielectric substrates, the scaled CSRR structure can efficiently absorb incident electromagnetic radiation and convert it into localized electrical energy through rectifying circuits, forming a metamaterial-based rectenna system.

Such a configuration enables continuous wireless power transfer to UAV platforms, where incident THz or optical energy beams can be dynamically directed using adaptive beamforming techniques. Beam steering allows the transmitted electromagnetic power to track the UAV position in real time, maintaining high power density at the receiver and enabling persistent operation without onboard energy storage limitations

2.5 Chapter Summary

This chapter presented a comprehensive review of metamaterials and metamaterial absorbers together with their operating principles and major applications. The historical development of metamaterials was reviewed beginning with the theoretical predictions of Veselago and the subsequent practical realizations introduced by Pendry and Smith. Fundamental metamaterial characteristics, including negative permittivity, negative permeability, and negative refractive index, were discussed to illustrate the unique electromagnetic behavior of artificially engineered structures.

The concept of metamaterial absorbers was then introduced, together with the theoretical foundations governing electromagnetic absorption. The relationships between absorption, reflection, and transmission coefficients were presented, highlighting the importance of impedance matching and resonant electromagnetic interactions in achieving near-perfect absorption.

Several representative metamaterial absorber applications were reviewed across different frequency ranges. Microwave absorbers were discussed in the context of radar cross-section reduction, wireless communications, and sensing systems. Terahertz absorbers were examined for imaging, spectroscopy, and sensing applications, while optical absorbers were reviewed with particular emphasis on photonic devices, thermal emission control, and solar energy harvesting systems. Furthermore, plasmonic metamaterial ab-

sorbers for UAV energy harvesting were introduced as an emerging application area with significant future potential.

The reviewed literature demonstrates that the electromagnetic response of metamaterial absorbers can be effectively controlled through geometrical design and resonance engineering. In particular, geometrically scalable resonators provide a practical mechanism for tuning resonance frequencies across different spectral regions. Moreover, multi-resonator configurations offer promising opportunities for achieving broadband absorption through resonance interaction and spectral overlap.

Based on these observations, the following chapter focuses on the implementation and re-simulation of selected metamaterial absorbers as well as the development of geometrically scaled optical double split ring resonator absorbers operating at different optical frequencies.

Chapter 3

Implementation and Re-simulation of Metamaterial Absorbers

3.1 Introduction

In this chapter, some Metamaterial absorbers are resimulated from literatures for the seek of verification. The realization of the extended perfect metamaterial absorbers in the optical band is then sophisticated.
The re-simulation process is performed using CST Microwave Studio to verify the performance of different metamaterial absorber structures reported in the literature. This step ensures that the simulation environment, boundary conditions, and material definitions are correctly implemented. Metamaterial absorbers operating at different frequency ranges, including microwave and terahertz bands, are investigated. The obtained results are compared with the published work to validate the accuracy of the modeling approach.

3.2 Basic Equations

The operation of the metamaterial absorber is governed by the electromagnetic interaction between the incident wave and the resonant structure. The absorption performance is evaluated using the scattering parameters, which describe the reflected and transmitted power. Since the absorber is backed by a metallic ground plane, the transmission is negligible, and the absorption can be expressed in terms of the reflection coefficient. In addition, the resonance behavior of the structure is determined by the equivalent inductance and capacitance of the resonator. The following equations are used to analyze the absorption characteristics and resonance properties of the proposed metamaterial absorber.

The fundamental resonance frequency is given by

$$f_0 = \frac{1}{2\pi\sqrt{L_{eq}C_{eq}}} \tag{3.1}$$

or equivalently,

$$L_{eq}C_{eq} = \frac{1}{(2\pi f_0)^2}. \tag{3.2}$$

The inductances of the outer and inner rings are approximated by

$$L_1 = \mu_0 r_1 \left[\ln\left(\frac{8r_1}{w}\right) - 2\right], \tag{3.3}$$

$$L_2 = \mu_0 r_2 \left[\ln\left(\frac{8r_2}{w}\right) - 2\right], \tag{3.4}$$

where

$$\mu_0 = 4\pi \times 10^{-7} \text{ H/m}. \tag{3.5}$$

The mutual inductance between the rings is

$$M \approx k\sqrt{L_1 L_2}, \tag{3.6}$$

with

$$0.6 < k < 0.95. \tag{3.7}$$

The equivalent inductance is

$$L_{eq} = L_1 + L_2 + 2M. \tag{3.8}$$

The split-gap capacitance is

$$C_g = \varepsilon_0 \varepsilon_r \frac{A}{g}, \tag{3.9}$$

where

$$A = w \times t, \tag{3.10}$$

and

$$\varepsilon_0 = 8.85 \times 10^{-12} \text{ F/m}. \tag{3.11}$$

Since the two gap capacitors are connected in series,

$$C_{g(\text{series})} = \frac{C_g}{2}. \tag{3.12}$$

The mutual capacitance between the rings is

$$C_m \approx \varepsilon_0 \varepsilon_r \frac{\pi r_{avg} t}{s}, \tag{3.13}$$

where

$$r_{avg} = \frac{r_1 + r_2}{2}. \tag{3.14}$$

The total capacitance is

$$C_{eq} = C_{g(\text{series})} + C_m. \tag{3.15}$$

3.3 Re-simulation of Metamaterial Absorber in Terahertz Band [53]

To further verify the modeling approach at higher frequencies, a terahertz broad-band metamaterial absorber reported in the second paper [53] is re-simulated. The structure consists of multiple metallic resonant rings separated from a metallic ground layer by a dielectric spacer as shown in the MTM absorber geometry in Fig. 3.1. This configuration enables impedance matching with free space, which minimizes reflection and enhances absorption.

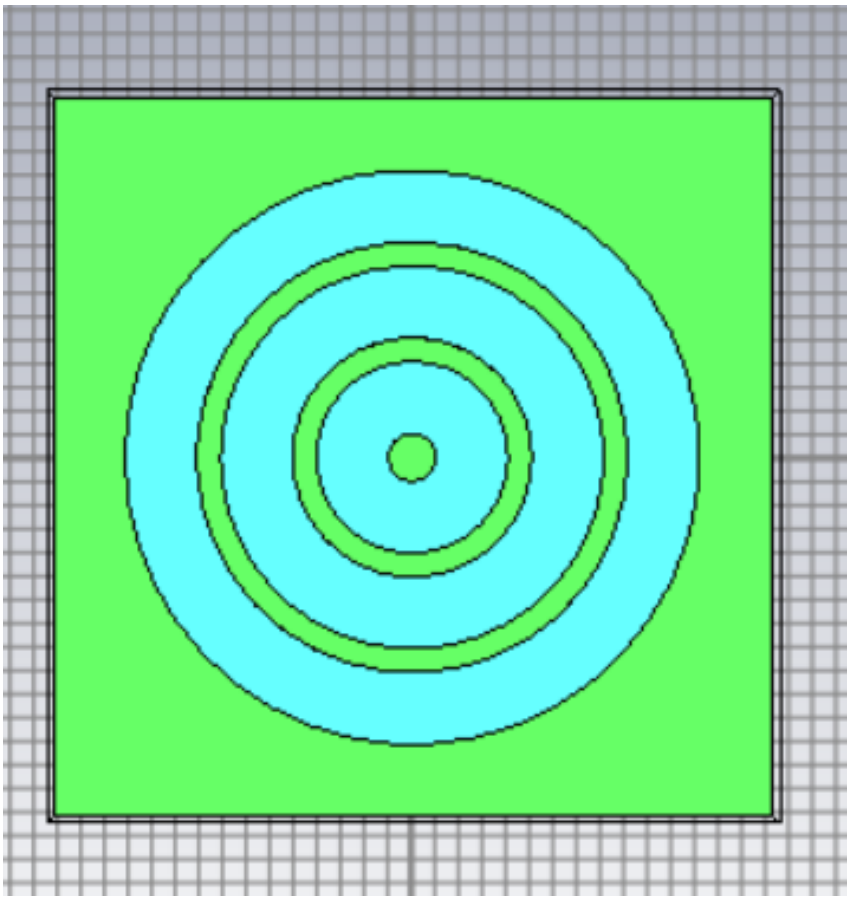
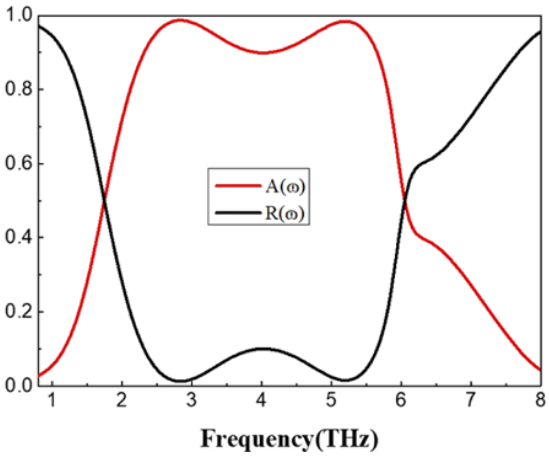


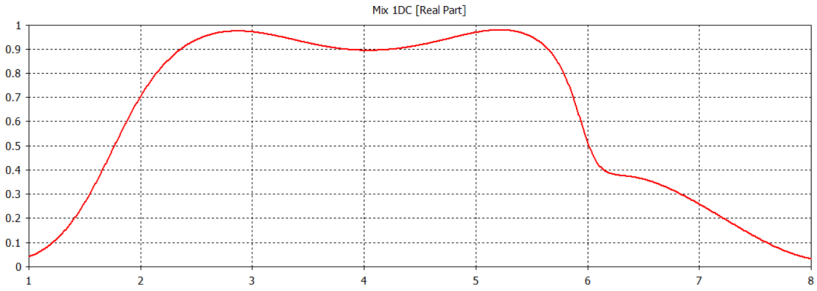
Figure 3.1: Unit cell geometry of the multi-ring terahertz metamaterial absorber [53].

According to the reference paper [53], the proposed absorber achieves broadband absorption greater than 90% over the frequency range from approximately 2.34 THz to 5.64

THz. The simulation is performed under normal incidence with periodic boundary conditions. The obtained results show a broadband absorbitivity from approximately 2.8 THz to 5.2 THz with values exceeds 90% over the same frequency range which showed a very good agreement with the reference paper [53] as illustrated in Fig. 3.2.



(a) reference [53]



(b) resimulated

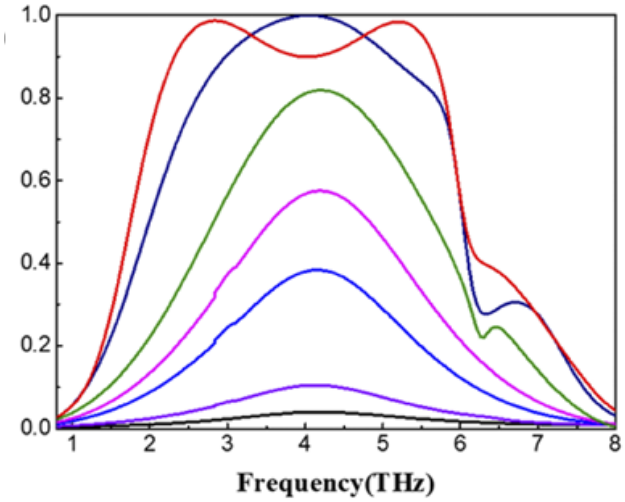
Figure 3.2: Absorbitivity of terahertz MTM absorber (a) reference [53] (b) resimulated.

Since the ground layer blocks transmission, the absorption is calculated using:

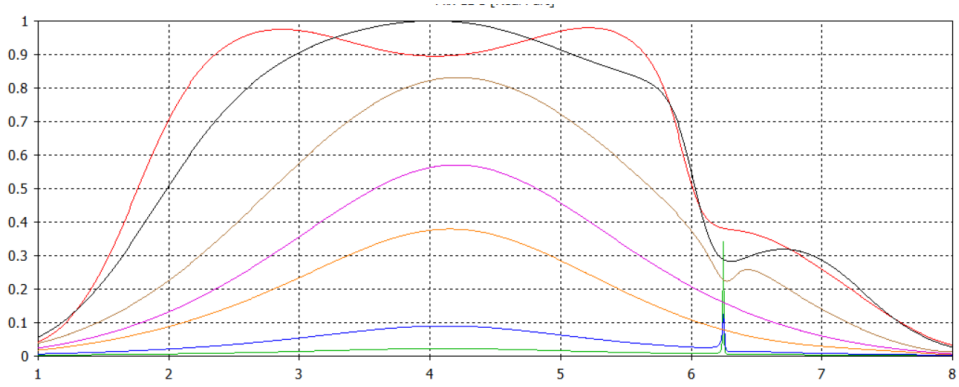
$$A(\omega) = 1 - |S_{11}|^2 \tag{3.16}$$

In the reference work [53], the absorption performance of the terahertz absorber is controlled by varying the electrical conductivity (σ) of the VO_2 layer. The conductivity is swept from 200 S/m (insulating state) to 2×10^5 S/m (metallic state). It is reported that the absorption increases gradually with increasing conductivity, reaching near-unity absorption at high conductivity values, while the operating frequency range remains nearly unchanged.

In this work, a similar conductivity sweep is performed over the same range. The obtained results show the same trend, where the absorption level increases with increasing conductivity and exceeds 90% within the operating frequency band at high conductivity values such comparison in presented in Fig. 3.3.



(a) reference [53]



(b) resimulated

Figure 3.3: Absorption variation of terahertz MTM absorber with conductivity (a) reference [53] (b) resimulated.

The results obtained in this work are in good agreement with those reported in [53], confirming the tunable behavior of the absorber and validating the accuracy of the CST re-simulation.

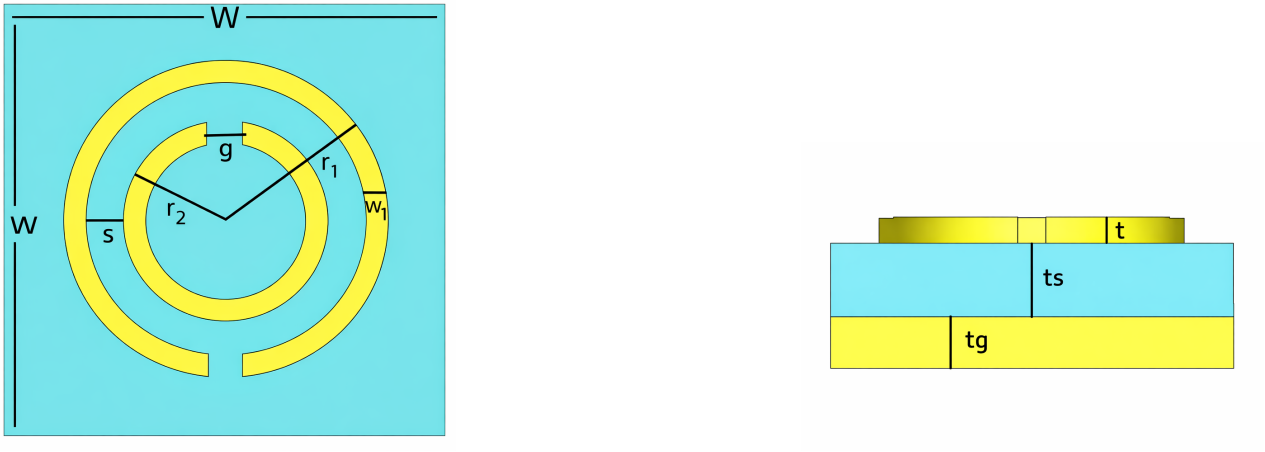
3.4 Development of Tunable MetaMaterial Absorber in Optical Band [54]

Metamaterial absorbers (MTMAs) have attracted significant attention due to their ability to achieve strong and selective electromagnetic absorption using subwavelength structures. They have garnered significant interest due to their unique electromagnetic features, which enable the efficient absorption of electromagnetic radiation in a specific frequency range or multiple frequency ranges. These absorbers are useful in many applications such as sensing, filtering, imaging, and photonic devices. Their designs are based on artificially engineered structures that enable tailored absorption properties [55–61].

They have been extensively researched due to their potential applications in photonics [56], [57], [59] Different designs have been proposed in the literature to achieve either broadband absorption or absorption at specific frequencies. Among these designs, split ring resonators (SRRs) and double split ring resonators (DSRRs) are widely used because they provide strong resonance behavior due to their inductive and capacitive properties, as well as their ability to operate across microwave, terahertz, and optical frequency regimes. In [56], a wideband near perfect light absorber in the midwave IR region using a multiplexed plasmonic metal structure is presented. The wideband near-perfect light absorber is made of two different size gold metal squares multiplexed on a thin dielectric spacing layer on top of a thick metal layer in each unit cell. A polarization insensitive and wide-angle broadband nearly perfect absorber by planar MTM in the visible regime is studied in [57]. The bandwidth of the absorption spectrum can be effectively expanded by combining multiple resonant elements. Shimaa I. Sayed et al. [59] designed a highly efficient broadband MTMA based on a Manganese–Silica–Manganese three-layer structure with a shaped pattern at the top layer for maximum absorption efficiency. Despite the large number of reported designs, most metamaterial absorbers are limited to fixed resonance frequencies that are determined once the geometry is defined. This makes it difficult to systematically control or tune the operating frequency without redesigning the entire structure. In addition, achieving multiple resonance frequencies using a single resonator remains challenging, as many existing approaches rely on combining different resonators or using complex geometries. Moreover, MTMAs are important for applications such as optical filtering, spectroscopy, sensing, and imaging. However, most of the existing work focuses either on fixed resonance frequencies or on broadband designs, with limited ability to systematically tune or control multiple resonances using a single structure. In many cases, different resonators are combined, or the design is optimized in a trial-and-error manner. In this work, a DSRR-based absorber is proposed and numerically investigated. The structure is designed to achieve resonances at multiple frequencies in the terahertz region through geometrical scaling without getting complicated structure. The electromagnetic response and underlying resonance mechanisms are analyzed using the FDTD CST Microwave Studio through the simulation of scattering parameters and surface current distributions. The paper is organized as follows: Section II presents the structure design, Section III illustrates the results and discussion, and the work is concluded in Section IV.

3.4.1 STRUCTURE DESIGN AND BASIC EQUATIONS

The proposed absorber consists of a double split ring resonator (DSRR) printed on a dielectric substrate. The structure is composed of three layers: a patterned metallic DSRR layer on the top, a dielectric spacer layer, and a continuous metallic ground plane



(a) (b)

Figure 3.4: Unit cell geometry of the proposed DSRR: (a) front view, (b) side view

at the bottom as illustrated in Fig.3.4.

The structure is composed of three layers: a patterned silver DSRR layer on the top, a dielectric spacer layer, and a continuous metallic ground plane (silver) at the bottom. The ground layer suppresses electromagnetic transmission, allowing the structure to operate as an efficient absorber. The substrate material of spacer is SiO2 has relative permittivity 3.9, thickness of quarter wavelength, and conductivity of 13.3 * 10^7S/m. Table 3.1 depicts the missing dimensions of DSRR.

The incident electromagnetic wave is modeled as a plane wave propagating normally to the metamaterial surface, with the electric field oriented parallel to the split gaps. Under this excitation, the electric field induces charge accumulation across the gaps, producing circulating surface currents along the rings.

The resonance frequency of the structure is determined by the effective inductance "L" of the metallic rings and the capacitance "C" introduced by the split gaps. The resonance condition follows the classical LC resonance relation:

$$f_0 = \frac{1}{2\pi\sqrt{LC}} \tag{3.17}$$

The absorptivity of the structure is calculated from the scattering parameters using the following relation:

$$A(\omega) = 1 - R(\omega) - T(\omega) \tag{3.18}$$

where $R(\omega)$ and $T(\omega)$ represent the reflection and transmission coefficients, respectively. Since the ground plane blocks transmission ($T \approx 0$), the absorptivity can be expressed as

$$A(\omega) = 1 - |S_{11}|^2 \tag{3.19}$$

By systematically adjusting the ring dimensions, gap width, and spacing between the

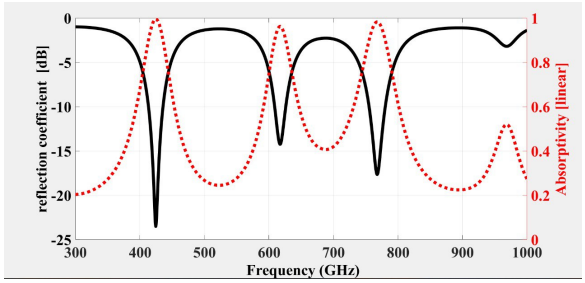
Table 3.1: Geometrical parameters of the proposed DSRR unit cell for different resonance frequencies.

Parameter	**423 THz (nm)**	**518 THz (nm)**	**640 THz (nm)**	**831 THz (nm)**
W	288	230.4	180	288
r_1	128	102.4	80	80
r_2	80	64	50	50
w_1	16	12.8	10	10
g_1	32	25.6	20	20
s	32	25.6	20	20
t_g	40	40	40	40
t_s	60	60	60	60
t	32	25.6	20	20

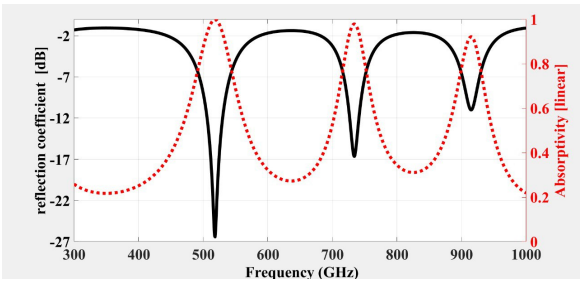
rings, the resonance frequency can be tuned across the optical frequency spectrum. The geometrical parameters used for the DSRR structure are summarized in Table 3.1.

3.4.2 Results and Discussion

Fig 3.5 shows the scattering parameters in terms of reflection coefficient and absorptivity of the proposed structure tuned at 423 THz and 518 THz. The simulated reflection coefficients for the designed structures demonstrate clear resonance dips at 423 THz, 518 THz. The depth of these dips indicates strong coupling between the incident electromagnetic field and the resonator with absorption 100% at both resonance. Surface current presented in Fig 3.6 for the case of 423 THz for explanation and confirmation of resonance (the color gradient from maximum to minimum is donted from red to light blue color). It confirms that the resonance mechanism is primarily driven by electric field induced charge accumulation at the split gaps, leading to circulating currents and energy confinement within the resonator.



(a) 423 THz



(b) 518 THz

Figure 3.5: Simulated reflection coefficient (S_{11}) and absorptivity of the proposed DSRR absorber at (a) 423 THz and (b) 518 THz.

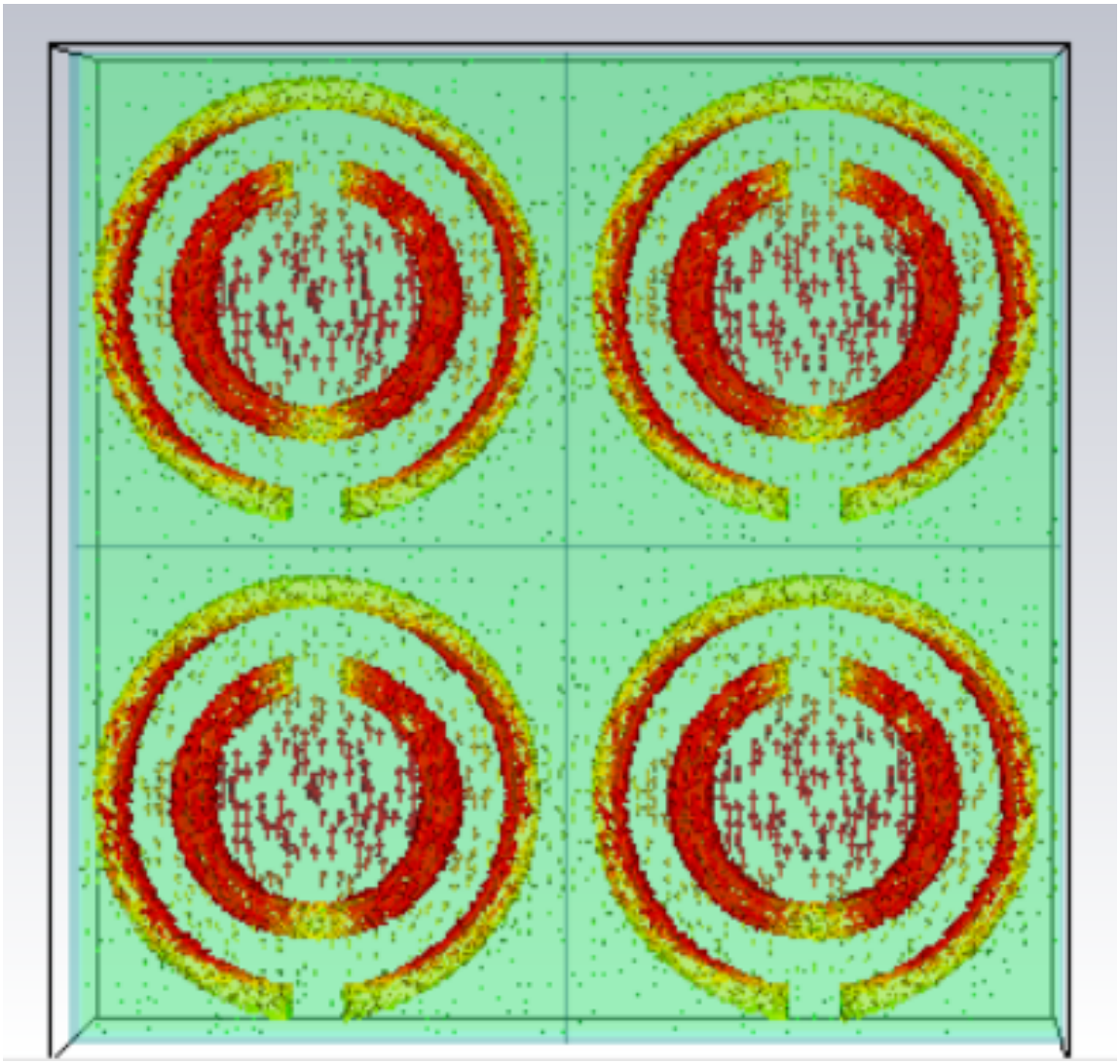
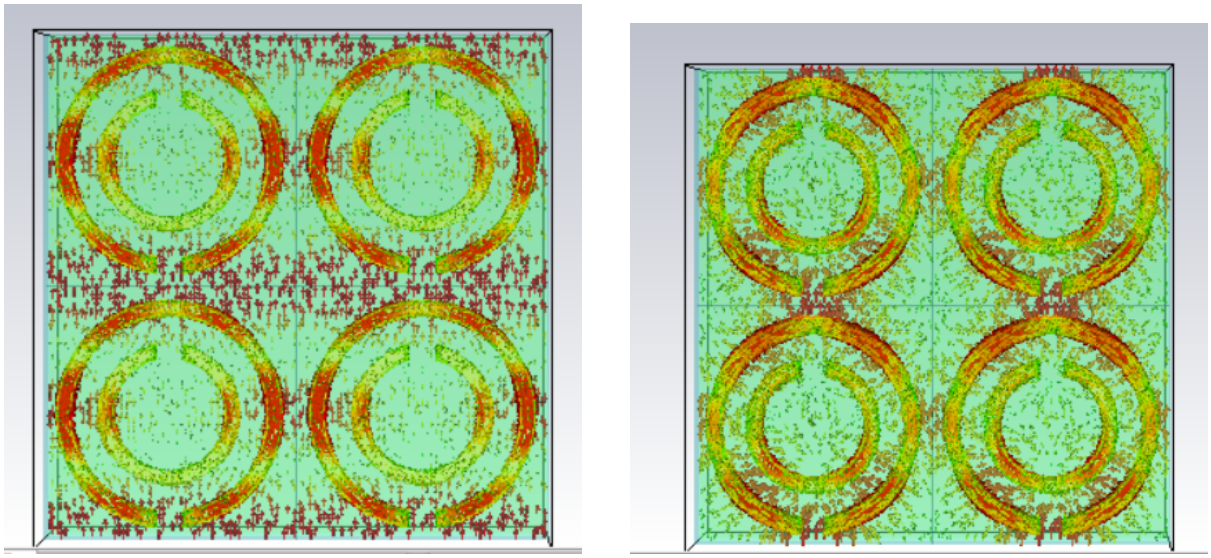


Figure 3.6: Surface current of the proposed DSRR absorber at 423 THz.

Also it is very important to point out that for the cases of 420 THz and 520 THz designs, multiple resonant dips are observed in the reflection spectrum as depicted in Fig 3.5. These additional resonances originate from higher order surface current modes supported

by the ring structure as well as electromagnetic coupling between the inner and outer rings. This can be confirmed if one see the surface current for the design at 420 THz which originates higher order mode resonance at 617.5 THz and 767 THz) due to the current maxima and nodes depicted at Fig 3.7 (surface current is gradient from red to light blue color).



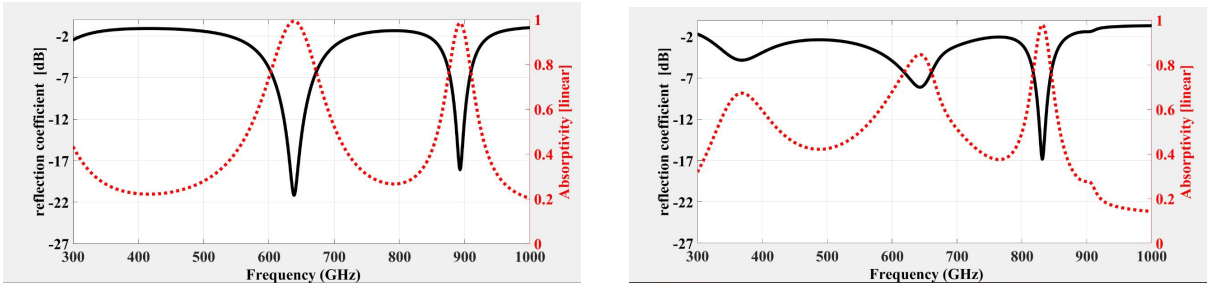
(a) 618 THz (b) 767 THz

Figure 3.7: Surface current of the proposed DSRR absorber at (a) 618 THz and (b) 767 THz.

Table 3.2: Comparison with previous works

Work	**Structure type**	**Resonance frequencies**	**Number of resonances**	**Peak absorption**	**Main tuning approach**
Wen et al. [62]	Electric split ring resonator (eSRR)	0.45 THz, 0.92 THz	2	Over 99.99% simulated; 80.8% and 63.4% measured	Different split gaps / dual LC resonances
Lu et al. [63]	Asymmetric DSRR	4.48 THz, 4.76 THz	2	98.6%, 98.5%	Gap asymmetry
This work	Geometrically scaled DSRR	423 THz, 518 THz, 640 THz, 831 THz	4	∼100%	Geometrical scaling

Similarly, Fig 3.8 illustrates the reflection coefficient and the absorption coefficient at 640 THz and 831 THz. At 640 THz, the fundamental resonance remains dominant, while a secondary resonance appears at higher frequencies. In contrast, the 831THz design exhibits only a single dominant resonance within the simulated frequency range. This behavior is mainly attributed to geometrical miniaturization of the resonator and increased material losses at higher frequencies, which suppress higher order resonant modes.



(a) 640 THz

(b) 831 THz

Figure 3.8: Simulated reflection coefficient (S_{11}) and absorptivity of the proposed DSRR absorber at (a) 640 THz and (b) 831 THz.

To further evaluate the proposed structure, a comparison is made with previously reported terahertz metamaterial absorbers. Wen et al. reported a dual-band terahertz metamaterial absorber with two distinct absorption points near 0.45 THz and 0.92 THz, where the absorber response is related to two LC resonances generated using an electric split ring resonator structure [62]. Although strong absorption was achieved, the design was limited to only two resonance bands. In another work, Lu et al. proposed an ultrathin terahertz dual-band absorber using an asymmetric double split ring resonator and obtained two almost equal strong absorption peaks at 4.48 THz and 4.76 THz with absorptivity of 98.6% and 98.5%, respectively [63]. In that design, the tuning process depends on introducing asymmetry by shifting the gap position.
Compared with these works, the proposed design achieves four resonance frequencies using the same DSRR concept through systematic geometrical scaling shown in Table 3.2. In addition, the absorption level in the proposed structure approaches 100% at the designed resonances, while the tuning mechanism is based on changing the physical dimensions of the resonator rather than introducing structural asymmetry or using more complex resonator arrangements. This gives a more direct relation between geometry and resonance behavior and makes the tuning process more predictable.

3.5 Chapter Summary

This chapter presented the implementation and re-simulation of selected metamaterial absorbers operating at terahertz and optical frequencies. A broadband terahertz metamaterial absorber reported in the literature was re-simulated using CST Microwave Studio to verify the adopted simulation methodology. The obtained results showed good agreement with the published work, confirming the accuracy of the simulation setup and the validity of the modeling approach.
In addition, a tunable optical metamaterial absorber based on geometrically scaled double split ring resonators (DSRRs) was investigated. By systematically scaling the resonator dimensions, the absorption response was tuned to multiple resonance frequencies at 423

THz, 518 THz, 640 THz, and 831 THz. The obtained results demonstrated near-perfect absorption at the designed resonance frequencies and confirmed the effectiveness of geometrical scaling as a simple and predictable tuning mechanism. Surface current distributions were analyzed to explain the resonance behavior and identify the fundamental and higher-order resonant modes responsible for the observed absorption characteristics.
The results presented in this chapter establish the foundation for the next stage of the research. Building upon the concept of geometrically scaled DSRRs, the following chapter investigates the development of wideband multi-resonance optical metamaterial absorbers based on composite configurations of multiple coupled resonators. The interaction between resonators of different dimensions is exploited to enhance spectral coverage, broaden the absorption bandwidth, and improve the overlap with the solar blackbody radiation spectrum for energy harvesting applications.

Chapter 4

Development of Wideband Multi-Resonance Optical Metamaterial Absorber Based on Composite Geometrically Scaled Multiple DSRRs

4.1 Introduction

Since the introduction of the first near-perfect metamaterial absorber by Landy *et al.* [64], metamaterial absorbers have been extensively investigated across microwave, terahertz, infrared, and optical frequency regimes. Their unique electromagnetic properties enable efficient suppression of reflection and transmission, allowing incident electromagnetic energy to be confined and dissipated within the structure. As a result, metamaterial absorbers have found numerous applications in optical sensing, thermal imaging, photodetection, thermal emission control, optical filtering, stealth technology, and solar energy harvesting [65].

The absorption behavior of metamaterial absorbers is primarily governed by the geometry of the resonant unit cell. Split ring resonators (SRRs) and double split ring resonators (DSRRs) are among the most widely used resonant structures due to their strong LC resonance characteristics, compact size, and high design flexibility. The resonance frequency of these structures can be controlled by modifying the geometrical dimensions of the metallic rings and split gaps, which directly affect the effective inductance and capacitance of the resonator. Consequently, DSRRs provide an effective platform for designing frequency-selective absorbers with tunable electromagnetic responses.

Although single-band absorbers can achieve near-unity absorption at specific frequencies, their narrow operating bandwidth restricts their usefulness in applications requiring broad spectral coverage. To overcome this limitation, numerous broadband and multi-

band metamaterial absorbers have been proposed. Hendrickson *et al.* [66] demonstrated broadband absorption by multiplexing metallic resonators with different dimensions, while Duan *et al.* [67] reported a broadband visible-frequency absorber based on planar metamaterial structures. Other studies have employed multi-resonator configurations, asymmetric resonators, hybrid metamaterial designs, and material-based optimization techniques to increase absorption bandwidth and improve spectral coverage [68–70].

Broadband optical absorption is particularly important for solar-energy-related applications. The solar blackbody radiation spectrum extends over a wide frequency range covering the visible and near-infrared regions. Therefore, absorbers designed for solar harvesting should maintain strong absorption over a broad spectral band rather than at isolated resonance frequencies. Achieving such behavior using a compact and geometrically simple metamaterial structure remains a challenging research problem. Ultra-broadband metamaterial absorbers have therefore been investigated as promising candidates for solar energy harvesting applications [71].

In the previous chapter, a geometrically scaled DSRR-based optical metamaterial absorber was developed to achieve tunable multi-frequency absorption [72]. By systematically varying the resonator dimensions, controlled absorption was demonstrated at multiple resonance frequencies ranging from 423 THz to 831 THz. Although near-perfect absorption was achieved at several frequencies, the generated resonances remained discrete and separated from one another, limiting the overall spectral coverage.

To overcome this limitation, this chapter extends the concept of geometrically scaled DSRRs by combining multiple resonators with different dimensions within a composite unit-cell configuration. Instead of using geometric scaling solely to tune isolated resonance frequencies, the proposed approach exploits electromagnetic coupling between neighboring resonators to generate additional resonant modes and promote spectral overlap. The interaction between resonators of different dimensions enables the gradual transition from discrete multi-frequency absorption to broadband absorption behavior.

The investigation is divided into two stages. First, two individual DSRR unit cells designed around 400 THz and 640 THz are investigated through parametric sweeps to verify the tunability of the resonator geometry. Second, composite structures consisting of two, three, and four coupled DSRR cells are introduced and analyzed to study resonance interaction, bandwidth evolution, and broadband absorption. Finally, a blackbody-weighted absorption analysis is performed to evaluate the ability of the proposed configurations to harvest solar radiation. The obtained results demonstrate that increasing the number of coupled resonators broadens the absorption bandwidth and enhances the overlap with the solar blackbody spectrum, resulting in improved harvesting performance.

4.2 Structure Design and Basic Equations

The proposed absorber consists of metallic DSRRs printed on a dielectric substrate backed by a continuous metallic ground plane. The metallic ground suppresses transmission, forcing the incident electromagnetic energy to be either reflected or absorbed.
The resonance frequency of the DSRR is governed by the equivalent inductance and capacitance of the resonator and may be approximated by

$$f_0 = \frac{1}{2\pi\sqrt{LC}} \tag{4.1}$$

where L represents the effective inductance and C represents the capacitance introduced by the split gaps.
The absorptivity is calculated using

$$A(\omega) = 1R(\omega)T(\omega) \tag{4.2}$$

Since the metallic ground suppresses transmission,

$$T(\omega) \approx 0 \tag{4.3}$$

Therefore, the absorptivity can be expressed as

$$A(\omega) = 1|S_{11}|^2 \tag{4.4}$$

The absorber performance is evaluated using CST Microwave Studio over the investigated optical frequency range.

4.3 Unit Cell Analysis

The geometry of the proposed single DSRR unit cell is illustrated in Fig. 4.1, where all geometrical parameters are indicated. The structure consists of two concentric splitring resonators printed on a dielectric substrate backed by a metallic ground plane. The geometrical dimensions of the resonator determine the effective inductance and capacitance of the structure and consequently control the resonance frequency and absorption behavior.

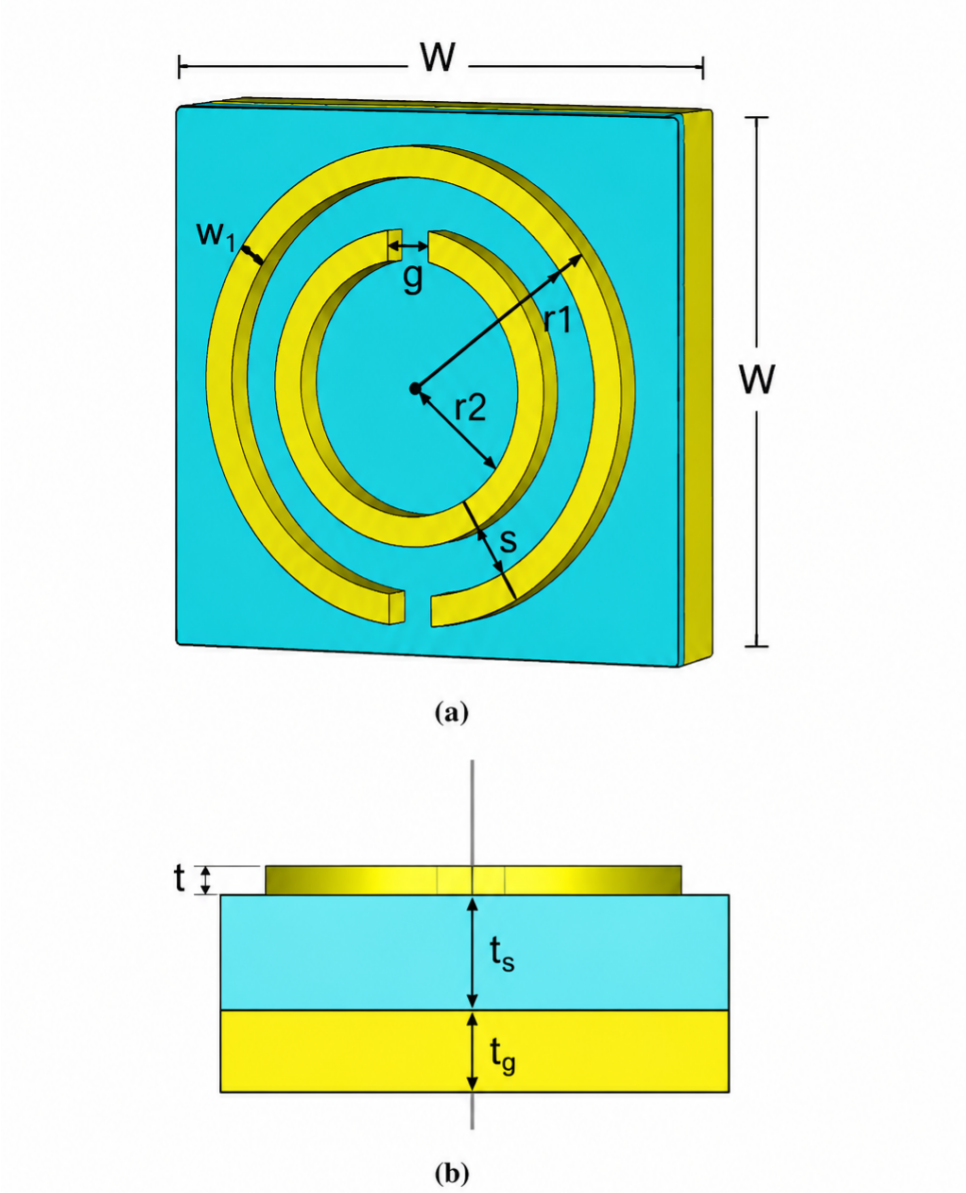


Figure 4.1: Geometry of the proposed single DSRR unit cell: (a) front view (b) side view

4.3.1 400 THz DSRR Unit Cell

The first stage of the investigation focuses on a DSRR unit cell designed around 400 THz. A parametric sweep is performed by varying the inner and outer ring radii as shown in Table 4.1.

Table 4.1: Geometrical Parameters of the 400 THz Unit Cell

Sweep	r_1 (nm)	r_2 (nm)
1	128	80
2	120	74
3	120	80

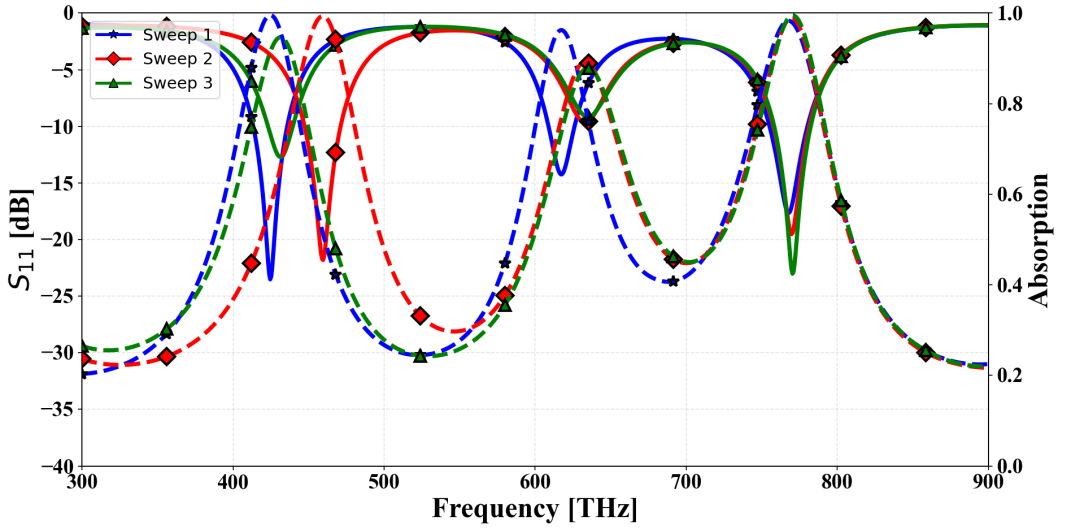


Figure 4.2: Reflection coefficient and absorptivity of the 400 THz unit cell for different geometrical sweeps.

The obtained results demonstrate that modifying the ring dimensions shifts the resonance frequencies and alters the absorption characteristics as illustrated in Fig. 4.2. The observed behavior confirms the dependence of the resonance frequency on the effective inductance and capacitance of the DSRR geometry.

4.3.2 640 THz DSRR Unit Cell

A second DSRR unit cell operating around 640 THz is investigated to demonstrate the tunability of the structure at a higher optical frequency the sweeping of the inner and outer radii are shown in Table 4.2.

Table 4.2: Geometrical Parameters of the 640 THz Unit Cell

Sweep	r_1 (nm)	r_2 (nm)
1	128	80
2	143	70
3	112	70

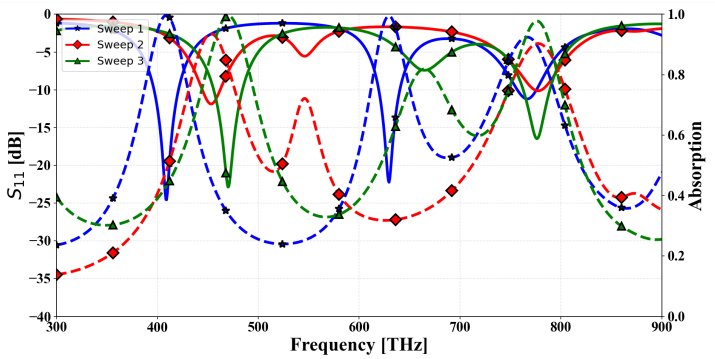


Figure 4.3: Reflection coefficient and absorptivity of the 640 THz unit cell for different geometrical sweeps.

The higher frequency unit cell exhibits similar tunability characteristics as shown in Fig. 4.3. Variations in the resonator dimensions modify the resonance locations and demonstrate the flexibility of DSRR structures for optical frequency engineering.

4.4 Composite Cell Analysis

4.4.1 Two Cell Configuration

The first composite structure combines two geometrically scaled DSRRs within a single unit cell. This configuration is used to investigate the initial interaction between two resonant elements. The proposed Two-Cell's configuration geometry is shown in Fig. 4.4, and the sweeping parameters is proposed in Table 4.3.

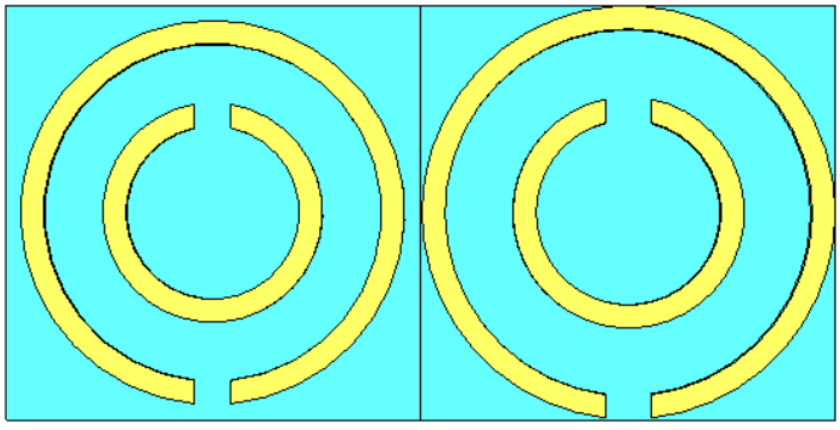


Figure 4.4: Geometry of the proposed two cell composite absorber.

Table 4.3: Geometrical Parameters of the Two Cell Configuration

Sweep	r_3 (nm)	r_4 (nm)
1	118	66
2	133	74
3	133	70

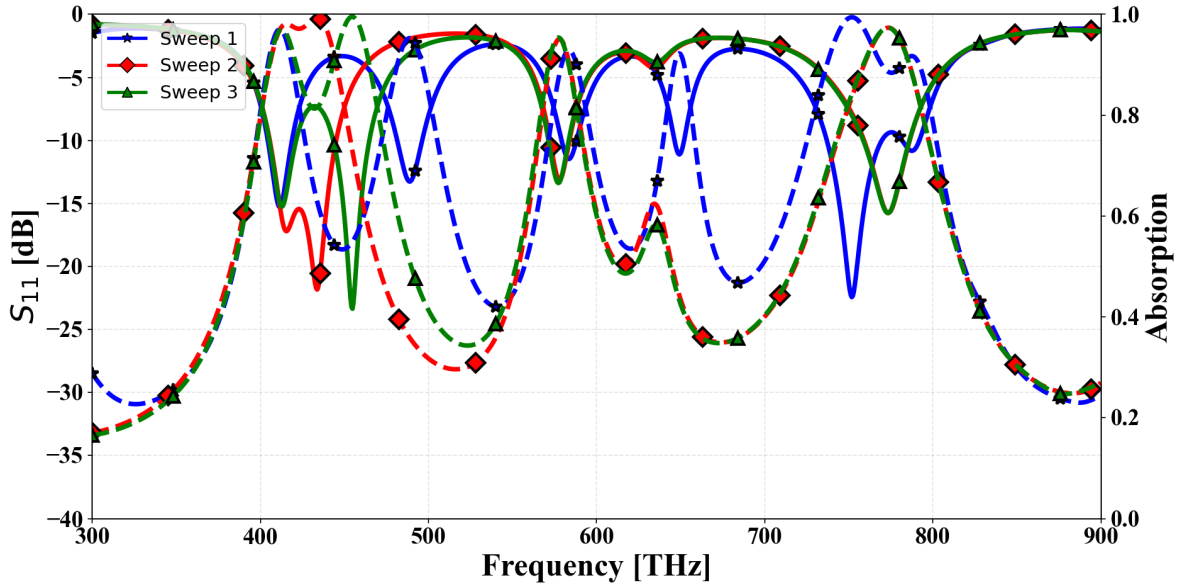


Figure 4.5: Reflection coefficient and absorptivity of the two cells composite absorber for different geometrical sweeps.

The introduction of a second resonator generates additional resonant modes and increases the spectral coverage as illustrated in Fig. 4.5 compared with the individual DSRR structures. This confirms that coupling between resonators can be used as an effective mechanism for bandwidth enhancement.

4.4.2 Three Cell Configuration

A third resonator is incorporated to increase the resonance density and promote stronger spectral overlap. The proposed Three-Cell's configuration geometry is shown in Fig. 4.6, and the sweeping parameters is proposed in Table 4.4.

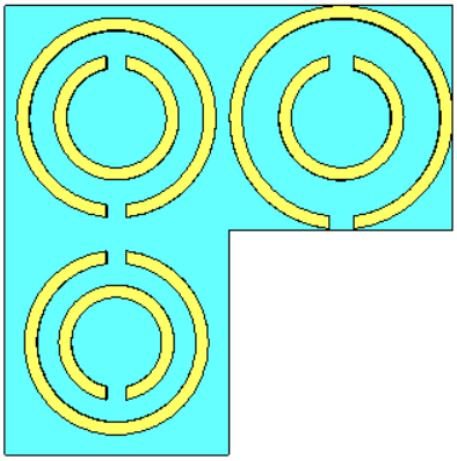


Figure 4.6: Geometry of the proposed three cell composite absorber.

Table 4.4: Geometrical Parameters of the Three Cell Configuration

Sweep	r_5 (nm)	r_6 (nm)	r_3 (nm)	r_4 (nm)
1	118	74	128	74
2	123	77	128	74
3	128	80	128	74

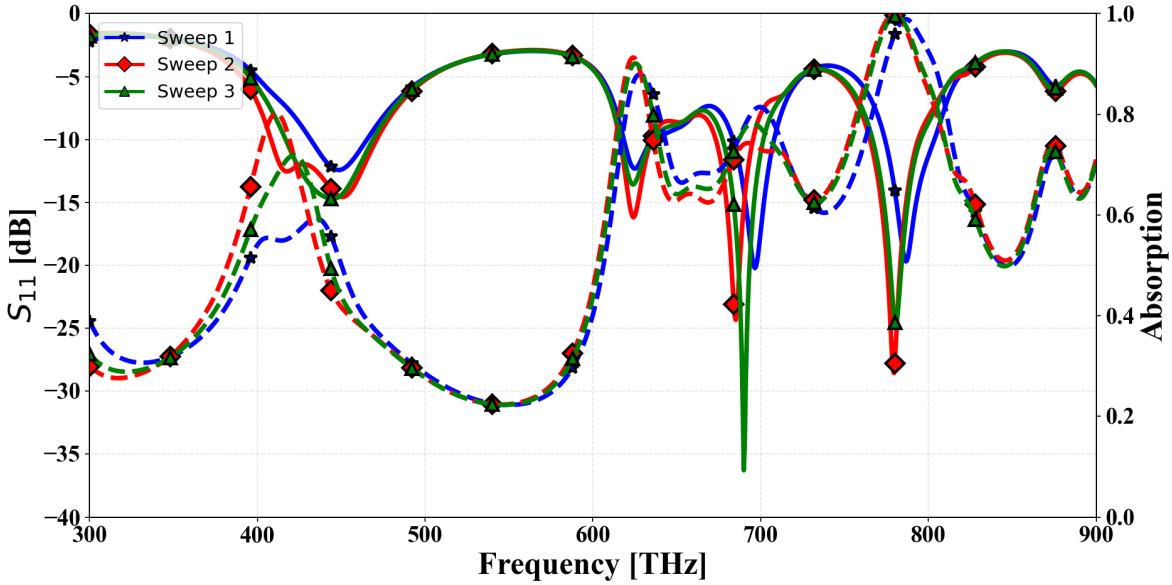


Figure 4.7: Reflection coefficient and absorptivity of the three cells composite absorber for different geometrical sweeps.

The interaction between the three resonators introduces additional coupled modes and promotes partial overlap between neighboring absorption bands. Compared with the

two cells configuration, the three cells structure provides a more continuous absorption response as illustrated in Fig. 4.7 .

4.4.3 Four Cells Configuration

The final configuration consists of four geometrically scaled DSRRs with the proposed geometry shown in Fig. 4.8. This structure represents the main wideband absorber proposed in this work. Table 4.5 represents the sweep of the multiradii of the proposed cells.

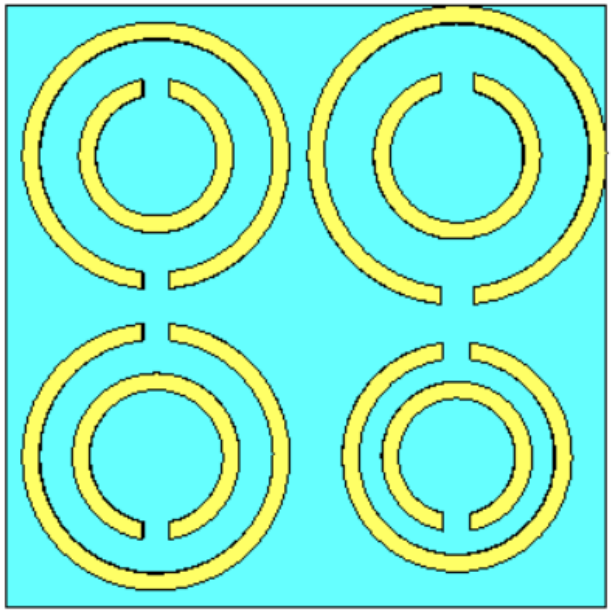


Figure 4.8: Geometry of the proposed four cells composite absorber.

Table 4.5: Geometrical Parameters of the Four Cells Configuration

Sweep	r_7 (nm)	r_8 (nm)	r_3 (nm)	r_4 (nm)
1	106	66	118	66
2	118	66	128	74
3	120	70	128	74

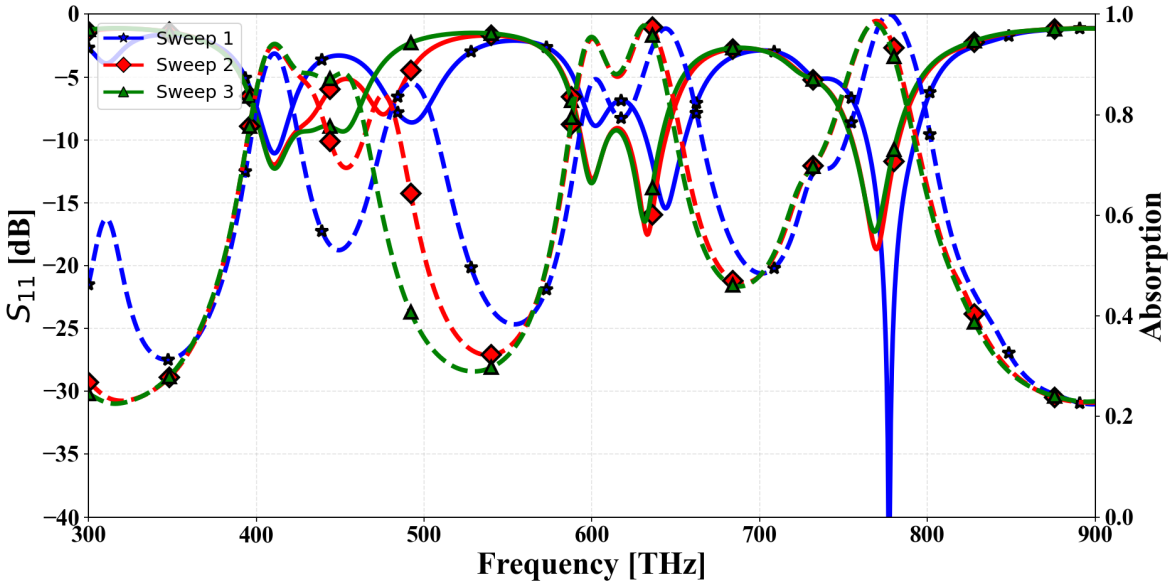


Figure 4.9: Reflection coefficient and absorptivity of the four cells composite absorber for different geometrical sweeps.

The four cells structure exhibits the strongest resonance interaction among all investigated configurations. Multiple resonant modes overlap and merge, producing a significantly broader absorption as illustrated in Fig. 4.9. This behavior demonstrates that increasing the number of geometrically scaled resonators enhances the spectral coverage of the absorber.

4.4.4 Broadband Absorption Mechanism

The observed bandwidth enhancement originates from the interaction between resonators of different dimensions. Each DSRR contributes a distinct resonance frequency. When several resonators are combined within the same structure, electromagnetic coupling generates additional hybrid modes. As the number of resonators increases, the resonance density becomes larger and neighboring resonances begin to overlap.
This resonance merging mechanism transforms the discrete absorption peaks observed in the individual unit cells into a broader absorption spectrum. Consequently, the four cells structure is capable of absorbing electromagnetic energy over a wider frequency range and can therefore interact with a larger portion of the solar blackbody radiation spectrum.

4.4.5 Blackbody Radiation Harvesting Analysis

The absorption spectra presented in the previous sections demonstrate that increasing the number of coupled resonators broadens the operating bandwidth of the metamaterial absorber. However, broadband absorption alone does not directly indicate the capability of the structure to harvest solar radiation. Therefore, a blackbody-weighted absorption

Table 4.6: Blackbody-Weighted Absorption Efficiency of the Investigated Configurations

Structure	**Sweep 1 (%)**	**Sweep 2 (%)**	**Sweep 3 (%)**	**Average (%)**
400 THz Unit Cell	48.51	48.68	48.06	**48.42**
640 THz Unit Cell	51.35	47.78	52.84	**50.65**
2 Cells	58.36	52.18	54.27	**54.94**
3 Cells	47.03	48.35	47.82	**47.73**
4 Cells	60.72	57.99	56.32	**58.34**

analysis was performed to quantify the fraction of the incident solar radiation that can be absorbed by each configuration. Since the Sun can be approximated as a blackbody radiator at a temperature of 5778 K, Planck's radiation law was employed to evaluate the overlap between the absorber response and the solar spectrum.
First Planck's blackbody spectral radiance:

$$B(f,T) = \frac{2hf^3}{c^2}\frac{1}{e^{hf/kT}-1} \tag{4.5}$$

where h is Planck's constant, c is the speed of light, k is Boltzmann's constant, f is the frequency, and T is the blackbody temperature.
The blackbody-weighted absorption efficiency is then calculated as:

$$\eta = \frac{\int_{f_1}^{f_2} A(f)\,B(f,T)\,df}{\int_{f_1}^{f_2} B(f,T)\,df} \times 100 \tag{4.6}$$

where A(f) denotes the absorptivity of the proposed metamaterial absorber and f1=300 THz and f2=900 THz define the investigated spectral range.
The calculated blackbody harvesting efficiencies for the individual resonators and the composite configurations are summarized in Table 4.6. For each structure, the efficiency was evaluated for the three investigated sweeps and the average value was subsequently determined. The obtained results provide a quantitative measure of the overlap between the absorption response and the solar blackbody spectrum.
The results reveal that the blackbody harvesting efficiency generally improves as additional resonators are incorporated into the absorber design. The four-cell configuration exhibits the highest average efficiency of 58.34%, indicating the strongest overlap with the solar blackbody spectrum over the investigated frequency range. In comparison, the individual 400 THz and 640 THz unit cells achieve average efficiencies of 48.42% and 50.65%, respectively. The enhanced performance of the four-cell structure is attributed to the generation of multiple resonant modes and the consequent bandwidth broadening, which enable a larger portion of the incident solar radiation to be absorbed. These findings

confirm that the proposed multi-resonator strategy is effective for improving broadband solar-energy harvesting performance.

4.5 Chapter Summary

This chapter presented the development of a wideband multi-resonance optical metamaterial absorber based on composite geometrically scaled double split ring resonators (DSRRs). Initially, individual DSRR unit cells operating around 400 THz and 640 THz were investigated through parametric sweeps to verify the dependence of the resonance response on the geometrical dimensions of the resonator.

Composite absorber configurations consisting of two, three, and four coupled DSRR cells were subsequently introduced and analyzed. The obtained results demonstrated that increasing the number of resonators within the unit cell generates additional resonant modes and promotes electromagnetic coupling between neighboring resonators. Consequently, the absorption bandwidth increased progressively as the number of coupled resonators increased. The four-cell configuration exhibited the strongest resonance interaction and achieved the broadest absorption response among all investigated structures.

The physical mechanism responsible for the observed bandwidth enhancement was also discussed. It was shown that each DSRR contributes a distinct resonance frequency, while electromagnetic coupling between resonators generates additional hybrid resonant modes. The overlap and merging of these resonances transform discrete absorption peaks into a broader absorption spectrum, thereby improving the spectral coverage of the absorber.

Finally, a blackbody-weighted absorption analysis was performed to evaluate the suitability of the proposed configurations for solar energy harvesting applications. The obtained results showed that the blackbody harvesting efficiency generally improves with increasing number of coupled resonators. The four-cell configuration achieved the highest average harvesting efficiency due to its enhanced bandwidth and stronger overlap with the solar blackbody radiation spectrum.

The results presented in this chapter demonstrate that composite geometrically scaled DSRR configurations provide an effective approach for realizing wideband optical metamaterial absorbers with improved solar energy harvesting capability.

Conclusion

This thesis presented the design, analysis, and optimization of optical metamaterial absorbers based on double split ring resonator (DSRR) structures for frequency-selective and broadband electromagnetic energy harvesting applications. The research was conducted through two complementary stages that progressively advanced the absorber performance

from controllable multi-frequency operation toward efficient wideband solar-spectrum absorption.

In the first stage, a geometrically scaled DSRR metamaterial absorber was developed and investigated to establish a direct relationship between resonator dimensions and resonance behavior. By systematically varying the geometrical parameters of the concentric split-ring structure, controlled absorption was achieved at multiple optical frequencies ranging from 423 THz to 831 THz. The study demonstrated that geometrical scaling provides a predictable and efficient tuning mechanism for resonance engineering while maintaining near-unity absorption at the desired frequencies. Furthermore, the analysis revealed the physical origin of higher-order resonances arising from electromagnetic coupling between the inner and outer rings, providing deeper insight into the resonance mechanisms governing optical metamaterial absorbers.

Building upon these findings, the second stage introduced composite configurations consisting of multiple geometrically scaled DSRRs integrated within a single unit cell. The objective was to transform discrete resonance peaks into a broadband absorption response through electromagnetic coupling and resonance merging. Numerical investigations of two-cell, three-cell, and four-cell configurations demonstrated that increasing the number of coupled resonators generates additional hybrid modes, enhances resonance density, and promotes spectral overlap. As a result, the absorption response evolved from isolated narrowband resonances into a significantly broader and more continuous spectral profile.

To evaluate the practical significance of the proposed structures for renewable-energy applications, a blackbody-weighted absorption analysis based on Planck's radiation law was performed. The results confirmed that broadband absorption directly improves the overlap between the absorber response and the solar blackbody radiation spectrum. Among all investigated designs, the four-cell composite absorber achieved the highest blackbody-weighted absorption efficiency of 58.34%, demonstrating the strongest capability for harvesting incident solar radiation within the investigated optical frequency range. These findings establish a clear link between resonance engineering, bandwidth enhancement, and solar-energy harvesting performance.

Overall, this thesis demonstrates that geometrical scaling and multi-resonator coupling provide a unified and scalable framework for engineering advanced optical metamaterial absorbers. The proposed designs successfully bridge the gap between frequency-selective absorption and broadband energy harvesting, offering a versatile platform for future applications in solar energy conversion, thermal photonics, selective thermal emitters, optical filtering, photodetection, sensing, and next-generation nanophotonic systems. The presented methodology also provides a foundation for future investigations involving adaptive metamaterials, tunable materials, artificial intelligence–assisted optimization, and experimentally realized ultrabroadband absorbers capable of approaching the theoretical limits of solar-radiation utilization

Future Work

Although the proposed metamaterial absorbers demonstrated excellent performance in terms of tunable multi-frequency absorption, wideband operation, and solar-radiation harvesting capability, several research directions remain open for further investigation.

Future work may include the fabrication and experimental characterization of the proposed DSRR-based metamaterial absorbers to validate the numerical results presented in this thesis. The influence of fabrication tolerances, material imperfections, and manufacturing limitations on the absorber performance can also be investigated.

Further enhancement of the absorption bandwidth may be achieved through the incorporation of additional resonators, fractal geometries, or hybrid metamaterial configurations. Alternative resonator topologies and novel unit-cell arrangements may also be explored to maximize resonance overlap and improve broadband absorption characteristics.

The integration of tunable and active materials such as graphene, phase-change materials, vanadium dioxide (VO_2), and other reconfigurable nanomaterials represents another promising research direction. Such materials may enable dynamic control of the absorption spectrum and facilitate the development of adaptive metamaterial absorbers capable of responding to changing environmental conditions.

In addition, optimization techniques based on artificial intelligence, machine learning, and evolutionary algorithms may be employed to automate the design process and identify optimal geometrical configurations for specific applications. These approaches can significantly reduce design complexity while improving absorber performance.

Future investigations may also focus on extending the proposed designs toward ultra-broadband absorbers with enhanced overlap with the solar blackbody radiation spectrum. Such developments could improve solar-energy harvesting efficiency and contribute to the realization of advanced photonic energy-conversion systems.

Finally, the proposed absorber structures may be adapted and optimized for a wide range of applications including thermal photovoltaics, selective thermal emitters, infrared camouflage, optical sensing, photodetection, thermal imaging, and next-generation nanophotonic devices.

Bibliography

[1] V. B. Bregar, A. Žnidarsic, D. Lisjak, and M. Drofenik, "Development and Characterisation of an Electromagnetic Absorber," *Materiali in Tehnologije*, vol. 39, no. 3, pp. 89–93, 2005.

[2] S. Li, X. Qiao, and J. Chen, "Nano-Composite Electromagnetic Wave Absorbers," *J. Astronautics*, vol. 2, 2006.

[3] V. G. Veselago, "The electrodynamics of substances with simultaneously negative values of ε and μ," *Soviet Physics Uspekhi*, vol. 10, no. 4, pp. 509–514, Jan.–Feb. 1968.

[4] J. B. Pendry, A. J. Holden, W. J. Stewart, and I. Youngs, "Extremely low frequency plasmons in metallic mesostructure," *Phys. Rev. Lett.*, vol. 76, no. 25, pp. 4773–4776, Jun. 1996.

[5] J. B. Pendry, A. J. Holden, D. J. Robbins, and W. J. Stewart, "Low frequency plasmons in thin-wire structures," *J. Phys.: Condens. Matter*, vol. 10, pp. 4785–4809, 1998.

[6] J. B. Pendry, A. J. Holden, D. J. Robbins, and W. J. Stewart, "Magnetism from conductors and enhanced nonlinear phenomena," *IEEE Trans. Microw. Theory Techn.*, vol. 47, no. 11, pp. 2075–2084, Nov. 1999.

[7] R. A. Shelby, D. R. Smith, and S. Schultz, "Experimental Verification of a Negative Index of Refraction," *Science*, vol. 292, no. 5514, pp. 77–79, 2001, doi:10.1126/science.1058847.

[8] J. B. Pendry, "Negative Refraction Makes a Perfect Lens," *Phys. Rev. Lett.*, vol. 85, no. 18, pp. 3966–3969, 2000, doi:10.1103/PhysRevLett.85.3966.

[9] A. A. Houck, J. B. Brock, and I. L. Chuang, "Experimental Observations of a Left Handed Material that Obeys Snell's Law," *Phys. Rev. Lett.*, vol. 90, no. 13, p. 137401, 2003, doi:10.1103/PhysRevLett.90.137401.

[10] D. R. Smith, W. J. Padilla, D. C. Vier, S. C. Nemat-Nasser, and S. Schultz, "Composite Medium with Simultaneously Negative Permeability and Permittivity," *Phys. Rev. Lett.*, vol. 84, no. 18, pp. 4184–4187, 2000, doi:10.1103/PhysRevLett.84.4184.

[11] D. R. Smith, W. J. Padilla, D. C. Vier, S. C. Nemat-Nasser, and S. Schultz, "Composite Medium with Simultaneously Negative Permeability and Permittivity," *Phys. Rev. Lett.*, vol. 84, no. 18, pp. 4184–4187, 2000, doi:10.1103/PhysRevLett.84.4184.

[12] R. M. Walser, "Electromagnetic Metamaterials," in *Complex Mediums II: Beyond Linear Isotropic Dielectrics*, vol. 4467, pp. 1–15, 2001.

[13] Y. I. Abdulkarim, A. Mohanty, O. P. Acharya, B. Appasani, M. S. Khan, S. K. Mohapatra, F. F. Muhammadsharif, and J. Dong, "A review on metamaterial absorbers: Microwave to optical," *Frontiers in Physics*, vol. 10, Art. no. 893791, 2022.

[14] Murata Manufacturing Co., Ltd., "What is a metamaterial?" [Online]. Available: `https://article.murata.com/en-global/article/what-is-a-metamaterial`. Accessed: Feb. 10, 2026.

[15] N. I. Landy, S. Sajuyigbe, J. J. Mock, D. R. Smith, and W. J. Padilla, "Perfect Metamaterial Absorber," *Phys. Rev. Lett.*, vol. 100, no. 20, p. 207402, 2008, doi:10.1103/PhysRevLett.100.207402.

[16] W. Zhang, F. Lan, J. Xuan, P. Mazumder, M. Aghadjani, Z. Yang, *et al.*, "Ultrasensitive Dual-Band Terahertz Sensing with Metamaterial Perfect Absorber," in *IEEE MTT-S Int. Microwave Workshop Ser. Adv. Mater. Process*, 2017, pp. 1–3, doi:10.1109/IMWS-AMP.2017.8247404.

[17] S. C. Bakshi, D. Mitra, and L. Minz, "A Compact Design of Multiband Terahertz Metamaterial Absorber with Frequency and Polarization Tunability," *Plasmonics*, vol. 13, no. 6, pp. 1843–1852, 2018, doi:10.1007/s11468-018-0698-2.

[18] M. Hedayati, F. Faupel, and M. Elbahri, "Review of Plasmonic Nanocomposite Metamaterial Absorber," *Materials*, vol. 7, pp. 1221–1248, 2014, doi:10.3390/ma7021221.

[19] A. Dubey and T. Shami, "Metamaterials in Electromagnetic Wave Absorbers," *Defence Science Journal*, vol. 62, no. 4, pp. 261–268, 2012, doi:10.14429/dsj.62.1514.

[20] B.-X. Wang, X. Zhai, G.-Z. Wang, W.-Q. Huang, and L.-L. Wang, "A Novel Dual-Band Terahertz Metamaterial Absorber for a Sensor Application," *J. Appl. Phys.*, vol. 117, no. 1, 2015, doi:10.1063/1.4905261.

[21] D. Li, H. Huang, H. Xia, Z. J., H. Li, and D. Xie, "Temperature-dependent Tunable Terahertz Metamaterial Absorber for the Application of Light Modulator," *Results in Physics*, vol. 11, pp. 659–664, 2018, doi:10.1016/j.rinp.2018.10.014.

[22] M. Yoo and S. Lim, "Polarization-Independent and Ultrawideband Metamaterial Absorber Using a Hexagonal Artificial Impedance Surface and a Resistor-Capacitor Layer," *IEEE Trans. Antennas Propag.*, vol. 62, no. 5, pp. 2652–2658, May 2014.

[23] V. G. Veselago, "The Electrodynamics of Substances with Simultaneously Negative Values of ε and μ," *Sov. Phys. Usp.*, vol. 10, no. 4, pp. 509–514, 1968, doi:10.1070/PU1968V010N04ABEH003699.

[24] N. I. Landy, S. Sajuyigbe, J. J. Mock, D. R. Smith, and W. J. Padilla, "Perfect Metamaterial Absorber," *Phys. Rev. Lett.*, vol. 100, no. 20, p. 207402, May 2008.

[25] J. Valentine, S. Zhang, T. Zentgraf, E. Ulin-Avila, D. A. Genov, G. Bartal, *et al.*, "Three-dimensional Optical Metamaterial with a Negative Refractive index," *Nature*, vol. 455, no. 7211, pp. 376–379, 2008, doi:10.1038/nature07247.

[26] J. Zhou, T. Koschny, M. Kafesaki, and C. M. Soukoulis, "Negative Refractive index Response of Weakly andStronglyCoupled Optical Metamaterials," *Phys. Rev. B*, vol. 80, no. 3, p. 035109, 2009, doi:10.1103/PhysRevB.80.035109.

[27] H. Guo, N. Liu, L. Fu, T. P. Meyrath, T. Zentgraf, H. Schweizer, *et al.*, "Resonance Hybridization in Double Split-Ring Resonator Metamaterials," *Opt. Express*, vol. 15, no. 19, pp. 12095–12101, 2007, doi:10.1364/OE.15.012095.

[28] D. Li, Y. Xie, J. Zhang, J. Li, and Z. Chen, "Multilayer Filters with Split-Ring Resonator Metamaterials," *J. Electromagn. Waves Appl.*, vol. 22, no. 10, pp. 1420–1429, 2008, doi:10.1163/156939308786348938.

[29] C. Shi, X.-F. Zang, Y. Wang, L. Chen, B. Cai, and Y. Zhu, "A Polarization-independent Broadband Terahertz Absorber," *Appl. Phys. Lett.*, vol. 105, p. 031104, 2014, doi:10.1063/1.4890617.

[30] J. Wang, S. Qu, Z. Xu, J. Zhang, H. Ma, Y. Yang, *et al.*, "Broadband Planar Left Handed Metamaterials Using Split-Ring Resonator Pairs," *Photon. Nanostruct. Fundam. Appl.*, vol. 7, no. 2, pp. 108–113, 2009, doi:10.1016/j.photonics.2009.01.001.

[31] Z. Li, Y. Ma, R. Huang, R. Singh, J. Gu, Z. Tian, *et al.*, "Manipulating the Plasmon Induced Transparency in Terahertz Metamaterials," *Opt. Express*, vol. 19, no. 9, pp. 8912–8919, 2011, doi:10.1364/OE.19.008912.

[32] D. Hu and H. Wang, "Design of Six-Band Terahertz Perfect Absorber Using a Simple U-Shaped Closed-Ring Resonator," *IEEE Photon. J.*, vol. 8, no. 2, p. 5500608, 2016, doi:10.1109/JPHOT.2016.2538758.

[33] G. Kenanakis, R. Zhao, N. Katsarakis, M. Kafesaki, C. M. Soukoulis, and E. N. Economou, "Optically Controllable THz Chiral Metamaterials," *Opt. Express*, vol. 22, no. 10, pp. 12149–12159, 2014, doi:10.1364/OE.22.012149.

[34] H. Zhang, F. Ling, H. Wang, Y. Zhang, and B. Zhang, "A Water Hybrid Graphene Metamaterial Absorber with Broadband Absorption," *Opt. Commun.*, vol. 463, p. 125394, 2020, doi:10.1016/j.optcom.2020.125394.

[35] Y. Qi, Y. Zhang, C. Liu, T. Zhang, B. Zhang, L. Wang, *et al.*, "A Tunable Terahertz Metamaterial Absorber Composed of Elliptical Ring Graphene Arrays with Refractive index Sensing Application," *Results in Physics*, vol. 16, p. 103012, 2020, doi:10.1016/j.rinp.2020.103012.

[36] C. Cen, Y. Zhang, X. Chen, H. Yang, Z. Yi, Y. Yao, *et al.*, "A Dual-Band Metamaterial Absorber for Graphene Surface Plasmon Resonance at Terahertz Frequency," *Physica E*, vol. 117, p. 113840, 2020, doi:10.1016/j.physe.2019.113840.

[37] C. Liu, L. Qi, and X. Zhang, "Broadband Graphene-Based Metamaterial Absorbers," *AIP Advances*, vol. 8, no. 1, p. 015301, 2018, doi:10.1063/1.4998321.

[38] S. K. Patel, S. Charola, C. Jani, M. Ladumor, J. Parmar, and T. Guo, "Graphene-based Highly Efficient and Broadband Solar Absorber," *Optical Materials*, vol. 96, p. 109330, 2019, doi:10.1016/j.optmat.2019.109330.

[39] R. Mishra, A. Sahu, and R. Panwar, "Cascaded Graphene Frequency Selective Surface Integrated Tunable Broadband Terahertz Metamaterial Absorber," *IEEE Photon. J.*, vol. 11, no. 2, pp. 1–10, 2019, doi:10.1109/JPHOT.2019.2900402.

[40] Y. Zhang, Y. Feng, B. Zhu, J. Zhao, and T. Jiang, "Graphene Based Tunable Metamaterial Absorber and Polarization Modulation in Terahertz Frequency," *Opt. Express*, vol. 22, no. 19, p. 22743, 2014, doi:10.1364/OE.22.022743.

[41] B. Hu, J. Tao, Y. Zhang, and Q. J. Wang, "Magneto-plasmonics in Graphene-Dielectric sandwich," *Opt. Express*, vol. 22, no. 18, pp. 21727–21738, 2014, doi:10.1364/OE.22.021727.

[42] H. Tao, N. I. Landy, C. M. Bingham, X. Zhang, R. D. Averitt, and W. J. Padilla, "A Metamaterial Absorber for the Terahertz Regime: Design, Fabrication and Characterization," *Opt. Express*, vol. 16, no. 10, pp. 7181–7188, 2008, doi:10.1364/OE.16.007181.

[43] B.-X. Wang, G.-Z. Wang, and L.-L. Wang, "Design of a Novel Dual-Band Terahertz Metamaterial Absorber," *Plasmonics*, vol. 11, no. 2, pp. 523–530, 2016, doi:10.1007/s11468-015-0076-2.

[44] A. Mohanty, O. P. Acharya, B. Appasani, and S. K. Mohapatra, "A Multi-Band Terahertz Metamaterial Absorber Based on a Π and U-Shaped Structure," *Photon. Nanostruct. Fundam. Appl.*, vol. 32, pp. 74–80, 2018, doi:10.1016/j.photonics.2018.10.008.

[45] J. Yang, C. Xu, S. Qu, H. Ma, J. Wang, and Y. Pang, "Optical Transparent Infrared High Absorption Metamaterial Absorbers," *J. Adv. Dielectrics*, vol. 8, no. 1, p. 1850007, 2018, doi:10.1142/S2010135X18500078.

[46] Y.-L. Liao and Y. Zhao, "Ultra-narrowband Dielectric Metamaterial Absorber with Ultra-sparse Nanowire Grids for Sensing Applications," *Sci. Rep.*, vol. 10, no. 1, pp. 1480–1487, 2020, doi:10.1038/s41598-020-58456-y.

[47] Y. Wang, Z. Chen, D. Xu, Z. Yi, X. Chen, J. Chen, *et al.*, "Triple-band Perfect Metamaterial Absorber with Good Operating Angle Polarization Tolerance Based on Split Ring Arrays," *Results in Physics*, vol. 16, p. 102951, 2020, doi:10.1016/j.rinp.2020.102951.

[48] F. Qin, Z. Chen, X. Chen, Z. Yi, Y. Yao, T. Duan, *et al.*, "A Tunable Triple-Band Near-Infrared Metamaterial Absorber Based on Au Nano-Cuboids Array," *Nanomaterials*, vol. 10, no. 2, p. 207, 2020, doi:10.3390/nano10020207.

[49] Z. Li, L. Stan, D. A. Czaplewski, X. Yang, and J. Gao, "Wavelength-selective Mid-infrared Metamaterial Absorbers with Multiple Tungsten Cross Resonators," *Opt. Express*, vol. 26, no. 5, pp. 5616–5631, 2018, doi:10.1364/OE.26.005616.

[50] Y. Avitzour, Y. A. Urzhumov, and G. Shvets, "Wide-angle Infrared Absorber Based on a Negative-index Plasmonic Metamaterial," *Phys. Rev. B*, vol. 79, no. 4, p. 045131, 2009, doi:10.1103/PhysRevB.79.045131.

[51] J. A. Bossard, L. Lin, S. Yun, L. Liu, D. H. Werner, and T. S. Mayer, "Near-Ideal Optical Metamaterial Absorbers with Super-octave Bandwidth," *ACS Nano*, vol. 8, no. 2, pp. 1517–1524, 2014, doi:10.1021/nn4057148.

[52] G. Wu, X. Jiao, Y. Wang, Z. Zhao, Y. Wang, and J. Liu, "Ultra-wideband tunable metamaterial perfect absorber based on vanadium dioxide," *Optics Express*, vol. 29, no. 2, pp. 2703–2710, Jan. 2021, doi: 10.1364/OE.416227.

[53] G. Wu, X. Jiao, Y. Wang, Z. Zhao, Y. Wang, and J. Liu, "Ultra-wideband tunable metamaterial perfect absorber based on vanadium dioxide," *Optics Express*, vol. 29, no. 2, pp. 2703–2710, Jan. 2021.

[54] M. N. Desouky, A. M. M. A. Allam, D. El-Damak, R. M. Elkhosht, D. E. Fawzy, and M. F. Abo Sree, "Tunable Multi-Frequency Optical Metamaterial Absorber Based on Geometrically Scaled Double Split Ring Resonators," in Proceedings of the IEEE ICEEE Conference, 2026.

[55] N. I. Landy, S. Sajuyigbe, J. J. Mock, D. R. Smith and W. J. Padilla, "A Perfect Metamaterial Absorber". 2008.

[56] Joshua Hendrickson, Junpeng Guo, Boyang Zhang, Walter Buchwald, and Richard Soref, "Wideband perfect light absorber at midwave infrared using multiplexed metal structures". Optical Letters, February 1, 2012 /Vol. 37, No. 3

[57] Xiaoyang Duan, Shuqi Chen, Wenwei Liu, Hua Cheng, Zhancheng Li and Jianguo Tian, Polarization-insensitive and wide-angle broadband nearly perfect absorber by tunable planar metamaterials in the visible Regime", Journal of optics, 16, 2014, doi:10.1088/2040- 8978/16/12/125107

[58] Mohammad S. Khan, S. K. Mohapatra, Fahmi F. Muhammad sharif and Jian Dong, "A Review on Metamaterial Absorbers:, Microwave to Optical", Frontiers of Phys. 10:893791. doi: 10.3389/fphy.2022.893791, 2022

[59] Shimaa I. Sayed, K. R. Mahmoud, and Roaa I. Mubarak 1, "Design and optimization of broadband metamaterial absorber based on manganese for visible applications", Scientific Report, doi.org/10.1038/s41598-023- 38263-x

[60] Anjie Cao, Nengfu Chen, Weiren Zhu, and Zhansheng Chen, "GrapheneBased Dual-Band Metasurface Absorber with High Frequency Ratio", nanomaterial, 2024

[61] Haiyu Zheng, Thanh Son Pham, Liangyao Chen and Youngpak Lee, "Metamaterial Perfect Absorbers for Controlling Bandwidth: SinglePeak/Multiple-Peaks/Tailored-Band/Broadband", 2024

[62] Q.-Y. Wen, H.-W. Zhang, Y.-S. Xie, Q.-H. Yang, and Y.-L. Liu, "Dual-band terahertz metamaterial absorber: Design, fabrication, and characterization," Applied Physics Letters, vol. 95, no. 24, p. 241111, 2009.

[63] T. Lu, D. Zhang, P. Qiu, J. Lian, M. Jing, B. Yu, and J. Wen, "Ultrathin terahertz dual-band perfect metamaterial absorber using asymmetric double-split rings resonator," Symmetry, vol. 10, no. 7, p. 293, 2018.

[64] N. I. Landy, S. Sajuyigbe, J. J. Mock, D. R. Smith, and W. J. Padilla, "Perfect Metamaterial Absorber," *Physical Review Letters*, vol. 100, no. 20, p. 207402, 2008.

[65] M. S. Khan, S. K. Mohapatra, F. F. M. Sharif, and J. Dong, "A Review on Metamaterial Absorbers: Microwave to Optical," *Frontiers in Physics*, vol. 10, p. 893791, 2022.

[66] J. Hendrickson, J. Guo, B. Zhang, W. Buchwald, and R. Soref, "Wideband Perfect Light Absorber at Midwave Infrared Using Multiplexed Metal Structures," *Optics Letters*, vol. 37, no. 3, pp. 371–373, 2012.

[67] X. Duan, S. Chen, W. Liu, H. Cheng, Z. Li, and J. Tian, "Polarization-Insensitive and Wide-Angle Broadband Nearly Perfect Absorber by Tunable Planar Metamaterials in the Visible Regime," *Journal of Optics*, vol. 16, no. 12, p. 125107, 2014.

[68] S. I. Sayed, K. R. Mahmoud, and R. I. Mubarak, "Design and Optimization of Broadband Metamaterial Absorber Based on Manganese for Visible Applications," *Scientific Reports*, vol. 13, 2023.

[69] A. Cao, N. Chen, W. Zhu, and Z. Chen, "Graphene-Based Dual-Band Metasurface Absorber with High Frequency Ratio," *Nanomaterials*, vol. 14, no. 1, 2024.

[70] H. Zheng, T. S. Pham, L. Chen, and Y. Lee, "Metamaterial Perfect Absorbers for Controlling Bandwidth: Single-Peak, Multiple-Peaks, Tailored-Band and Broadband," *Advanced Optical Materials*, vol. 12, 2024.

[71] M. Bagmanci, M. Karaaslan, E. Unal, O. Akgol, and C. Sabah, "Solar Energy Harvesting with Ultra-Broadband Metamaterial Absorber," *International Journal of Modern Physics B*, vol. 33, no. 08, p. 1950056, 2019.

[72] M. N. Desouky, A. M. M. A. Allam, D. El-Damak, R. M. Elkhosht, D. E. Fawzy, and M. F. Abo Sree, "Tunable Multi-Frequency Optical Metamaterial Absorber Based on Geometrically Scaled Double Split Ring Resonators," in *Proceedings of the 13th International Conference on Electrical and Electronics Engineering (ICEEE)*, Antalya, Turkey, 2026.